Diffraction, Microscopy and Spectroscopy at solid-liquid interfaces

Electric double layer

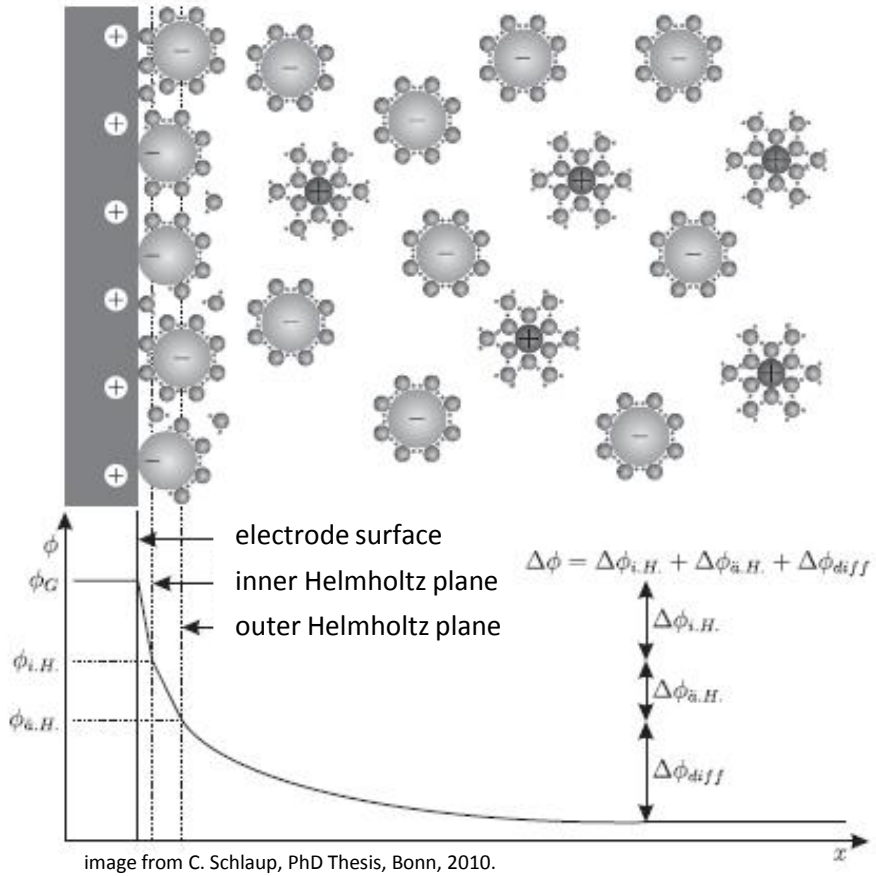

image from C. Schlaup, PhD Thesis, Bonn, 2010.

Inner Helmhotz plane:
Specifically adsorbed ions (inner sphere complexes) chemical bonding with surface; lost part of their solvation H_2O.

Outer Helmholtz plane:
Non-specifically adsorbed ions (outer sphere complexes)
Eleectrostatic interaction with surface completely solvated

A 1 V potential drop across the metal/ electrolyte interface leads to high surface charges (0.1-0.2 e per surface atom) and high electric fields (10^{-7} V/cm)

Metals: are charged by applying a potential
Minerals, oxides: charge results from pH dependent protonation/ deprotonation of surface hydroxyl groups.

Cyclic voltammetry

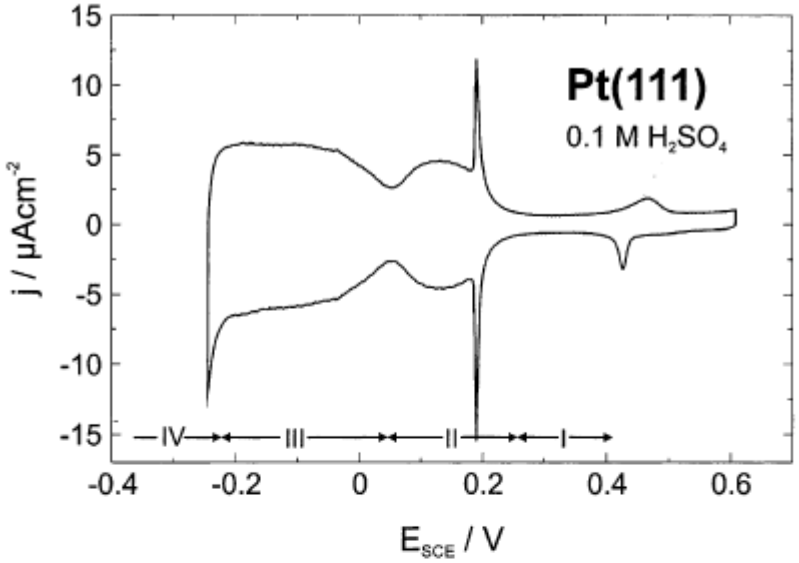

Fig. 2. CV for a Pt(1 1 1) electrode in 0.1 M H_2SO_4, recorded at a scan rate $dE/dt = 10\ mV\ s^{-1}$. CVs in general show the electric current as a function of electrode potential while the latter is continuously changed at constant scan rate back and forth within a given potential range. They yield fingerprints of the processes occurring at the electrode–electrolyte interface. In this CV, four different processes can be envisaged, the corresponding potential ranges being marked by roman numbers. No. I denotes the so-called double-layer charging region, where no electrochemical reaction (i.e., no charge transfer through the interface) takes place and where the "Helmholtz capacitor" is simply charged or discharged by the potential variation. No. II shows the region where sulfate adsorption takes place on the positive potential scan (desorption on the negative scan), while no. III comprises the region of hydrogen adsorption (atomic hydrogen!) and desorption during the negative and the positive scan, respectively. In region no. IV, hydrogen evolution causes a steep rise of the cathodic current.

from D. M. Kolb, Surf. Sci. 500 (2002) 722.

Surface Science:

Single crystal samples
Ultrahigh vacuum (10^{-10} mbar)
Surface structure
Electronic properties
Adsorption sites
Geometry of adsorbed species

WATER ???

Electrochemistry

Heterogeneous catalysis

Environmental Sciences

Biology

Methods:

Microscopy:
Scanning tunneling microscopy
Atomic force microscopy

Diffraction and scattering:
Low energy electron diffraction
Low energy ion scattering

Electron spectroscopy:
X-ray photoelectron spectroscopy
UV photoelectron spectroscopy
Auger electron spectroscopy
Electron energy loss spectroscopy

Optical spectroscopy:
IR spectroscopy

and many more

Electrochemical Surface Science:

the presence of water limits the application of surface science methods to:

optical methods (photon in – photon out)
local probe microscopy

Surface X ray diffration

Scanning probe microscopies

Infrared spectroscopy

Surface X-ray scattering techniques – Basic concepts

3D scattering

Miller indices

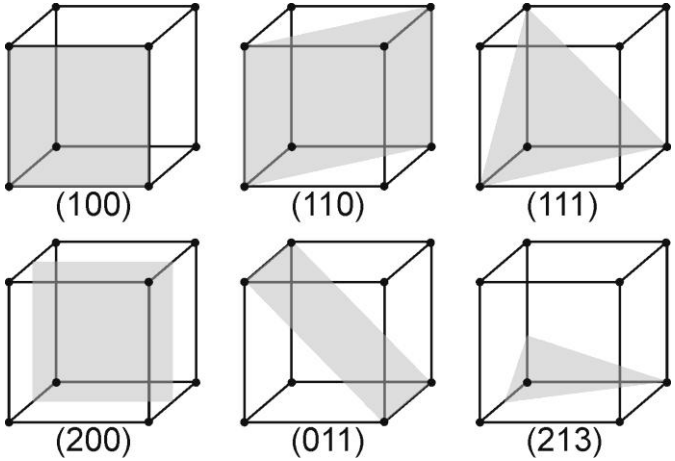

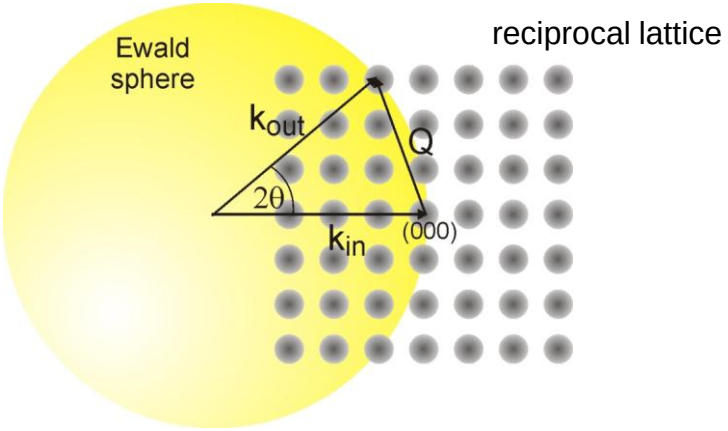

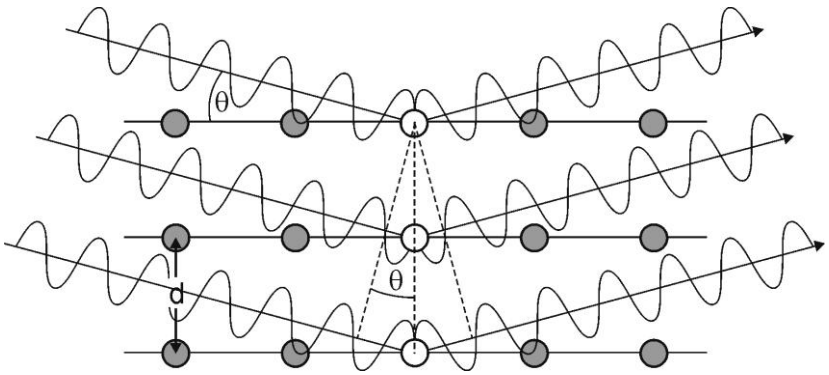

Bragg Law: $k_{in} = k_{out} = \frac{2\pi}{\lambda}$

$m\lambda = 2d \sin\theta$ $\quad \Delta k = \mathbf{Q}$

$|Q| = \frac{2\pi}{d_{hkl}}$ $\quad \mathbf{Q} = 2|k|\sin\theta = \frac{4\pi}{\lambda}\sin\theta$

$\Rightarrow$ lattice periodicity

Scattering amplitude (reciprocal space) $\Leftrightarrow$ (FT) Electron density (real space)

⇧

Structure factor F_{hkl}

⇧

Atomic scattering factor f

Surface X-ray scattering techniques – Basic concepts

Crystal truncation rods - CTR

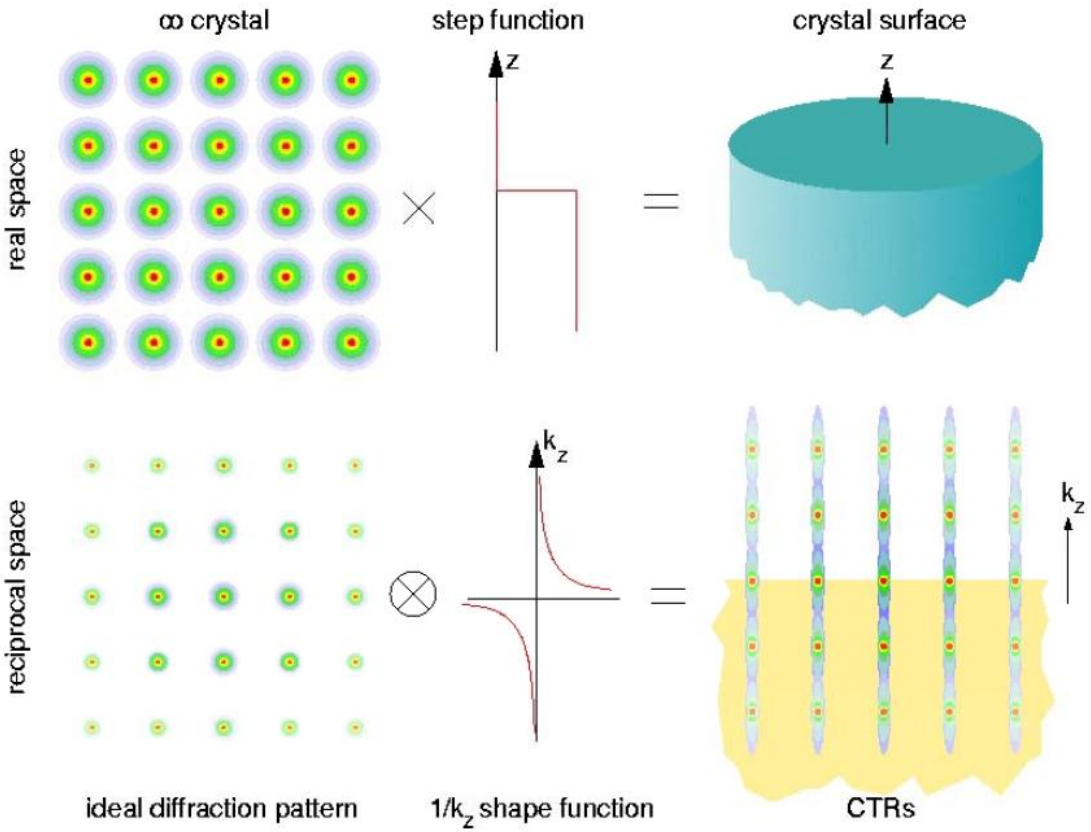

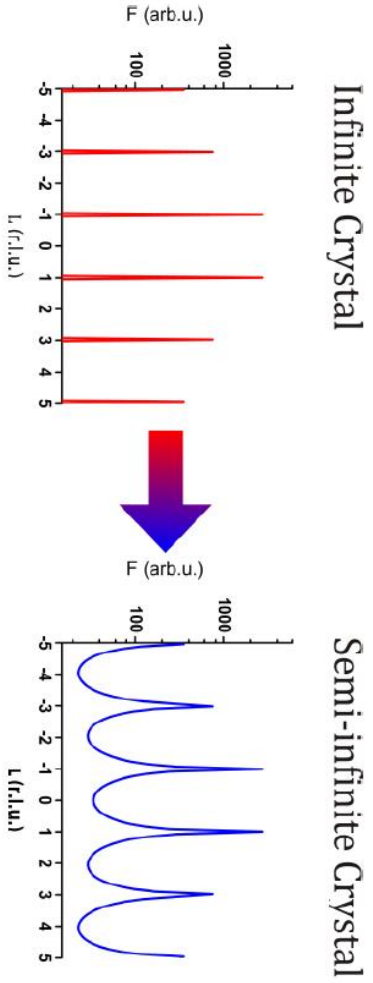

From P. Willmott, *An Introduction to Synchrotron Radiation: Techniques and Applications*, Wiley, 2011.

Specular Reflectivity

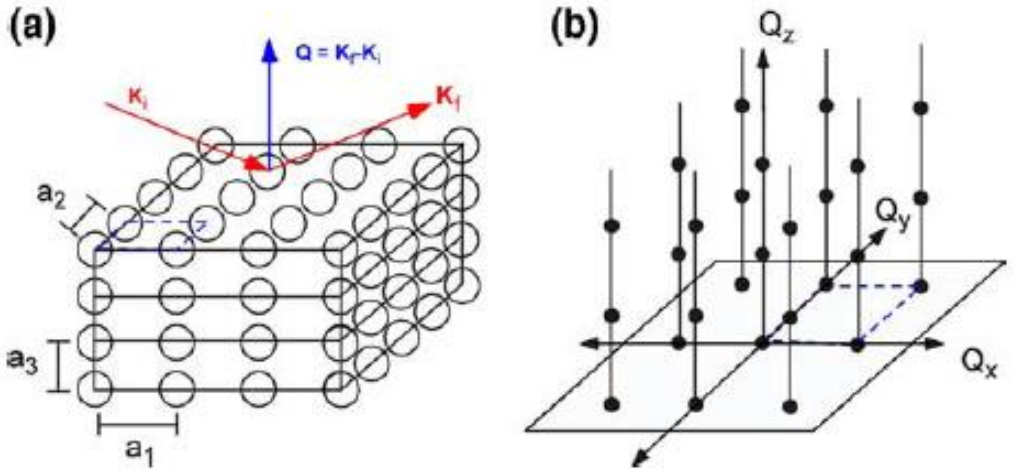

Surface X-ray diffraction

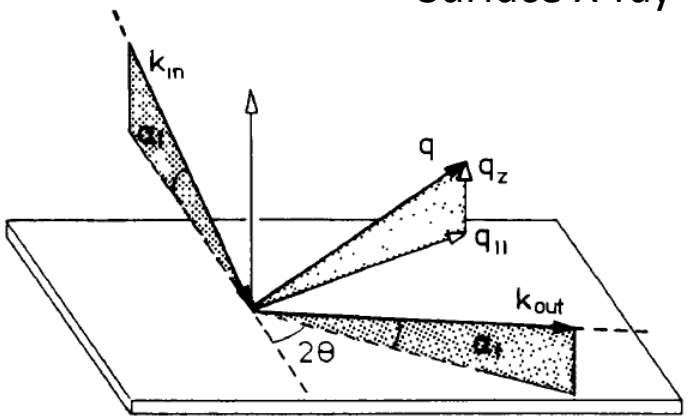

Fig. 2. Glancing angle geometry. The X-ray beam impinges onto the surface at an angle α_i. After diffraction through an angle 2θ the X-rays exit the surface at an angle α_f. Both α_i and α_f are typically $\sim 0.5°$ for in-plane studies. The momentum transfer q is composed of an in-plane component $q_{\|}$ and a component q_z normal to the surface

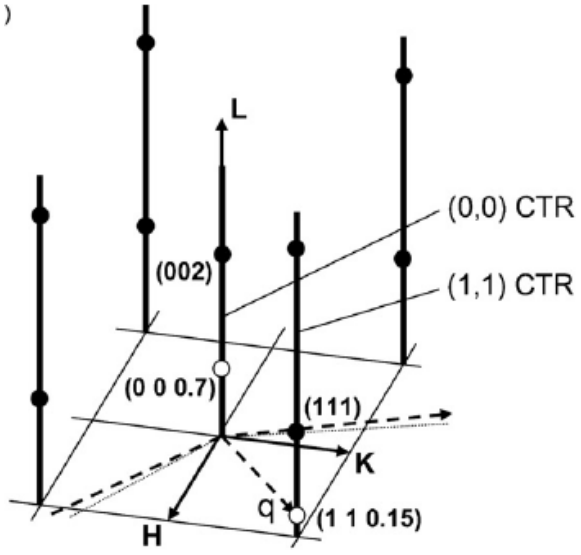

Surface X-ray scattering techniques – Basic concepts

ideal termination

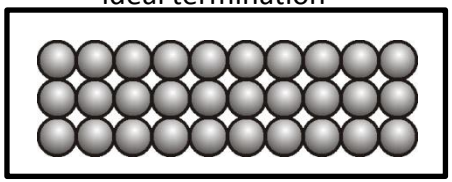

relaxation of 1st layer

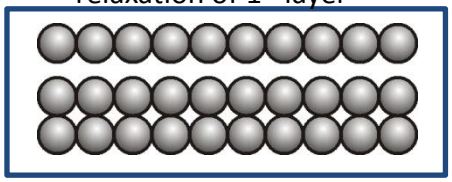

1st layer occupation

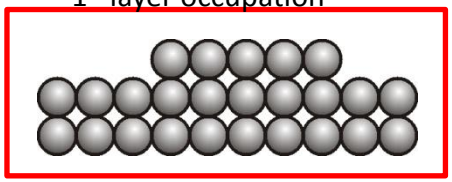

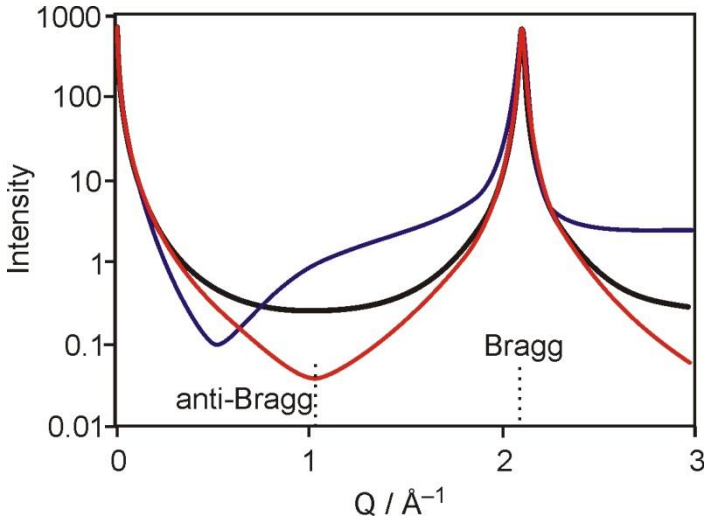

ordered superstructure
e.g. surface reconstruction

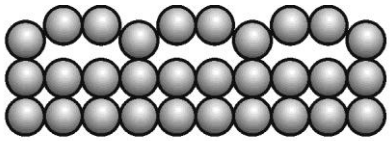

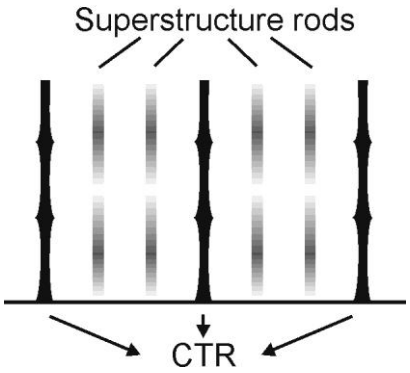

Surface X-ray scattering techniques – Basic concepts

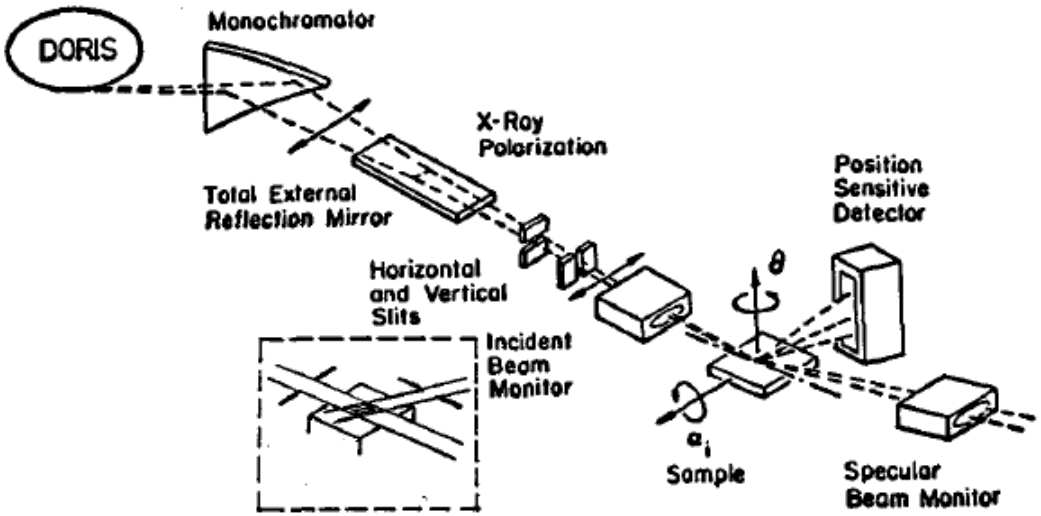

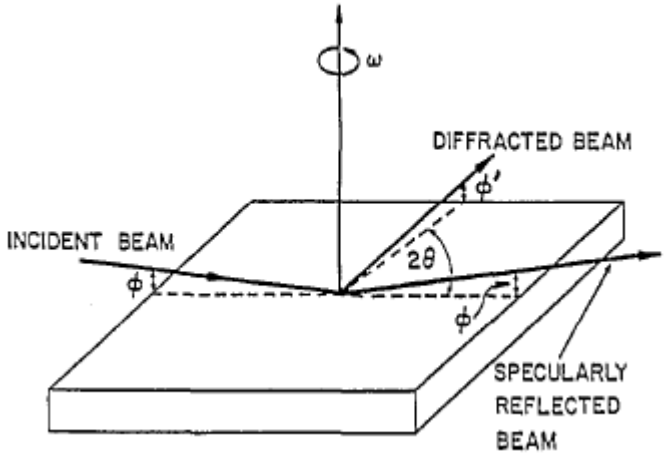

SXRS of solid liquid interfaces – sample cells

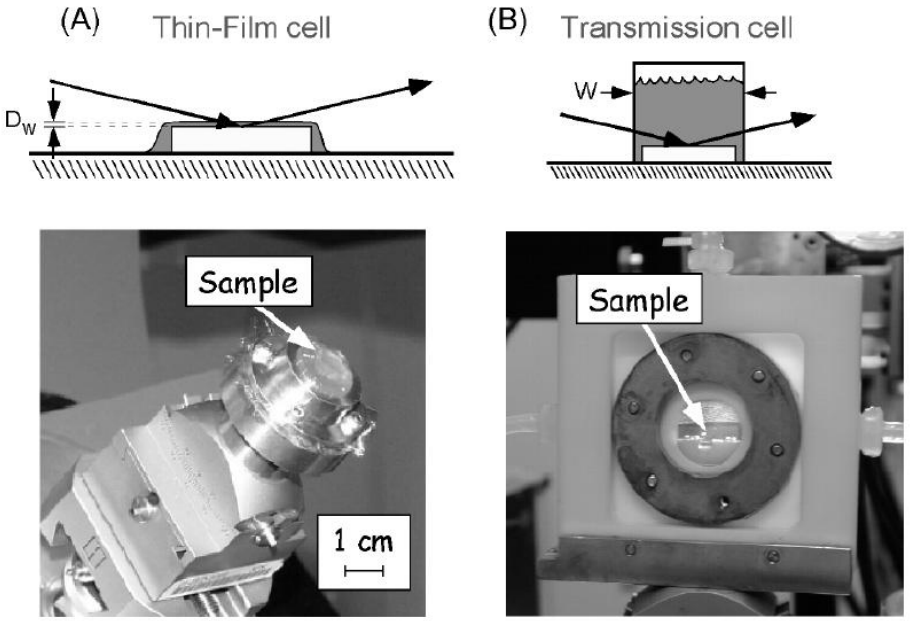

Figure 8. Schematic and photograph of the (A) thin-film and (B) transmission cell designs. The water film thickness, D_w, and cell width, W, for the two cell designs are shown.

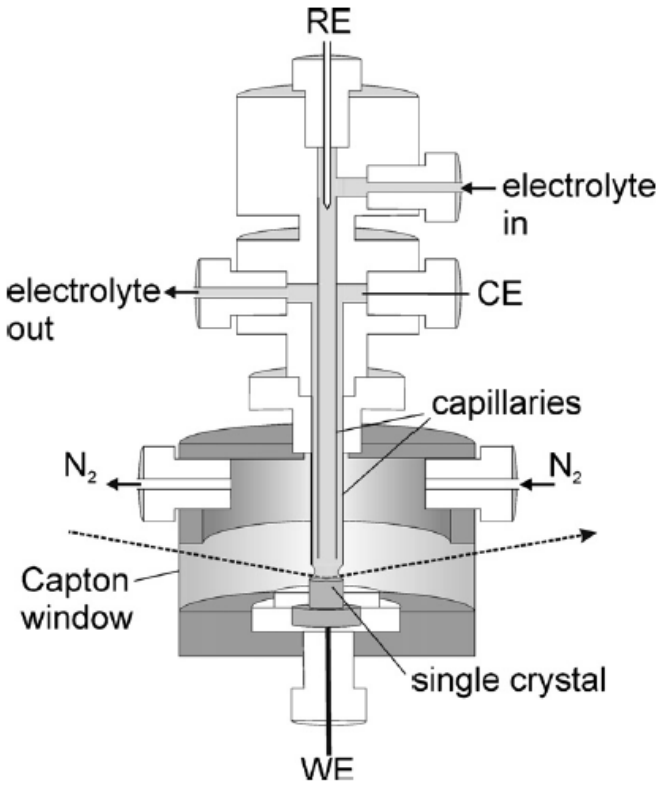

Fig. 1. Schematic drawing of the "hanging meniscus" transmission surface X-ray scattering cell. The dashed line indicates the X-ray beam.

Fenter, Int. Geochem Rev.

Magnussen et al. Electrochim. Acta 53 (2008) 3449.

SXRS – Examples

Au(111) (23×√3) → (1×1) phase transition

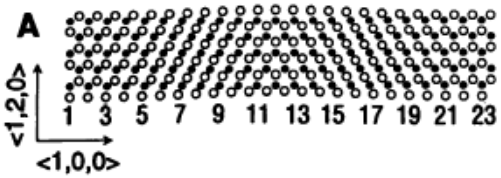

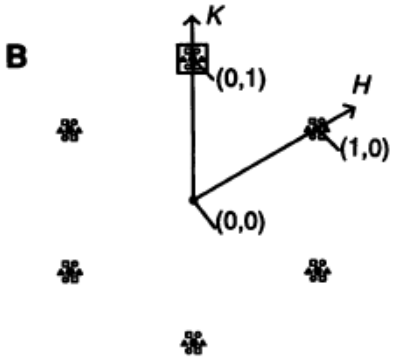

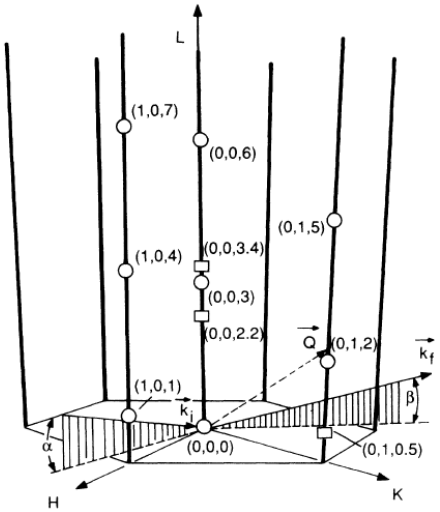

"Herringbone" reconstruction

J. Wang et al., Phys. Rev. B 46 (1992) 10321.

SXRS – Examples

Au(111) (23×√3) → (1×1) phase transition

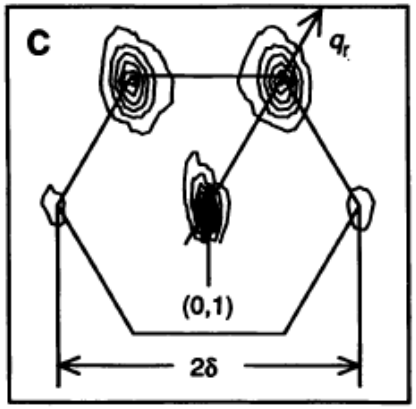

iso-intensity scattering contours in the vicinity of the (0,1) reflection

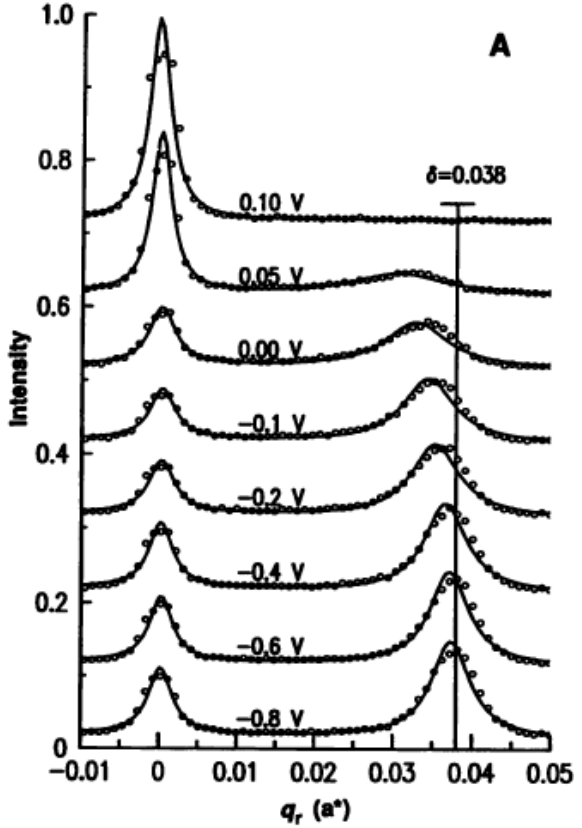

> 0.1 V: surface is not reconstructed
< 0.05 V: reconstructed phase

Peak moves outward and sharpens
→ increased compression and order

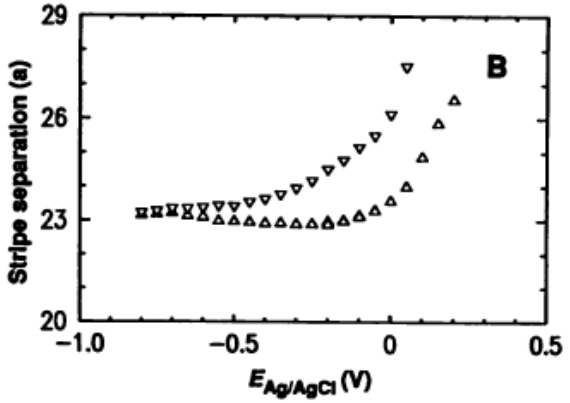

J. Wang et al., Phys. Rev. B 46 (1992) 10321.

SXRS – Examples

Au(111) electrochemical dissolution

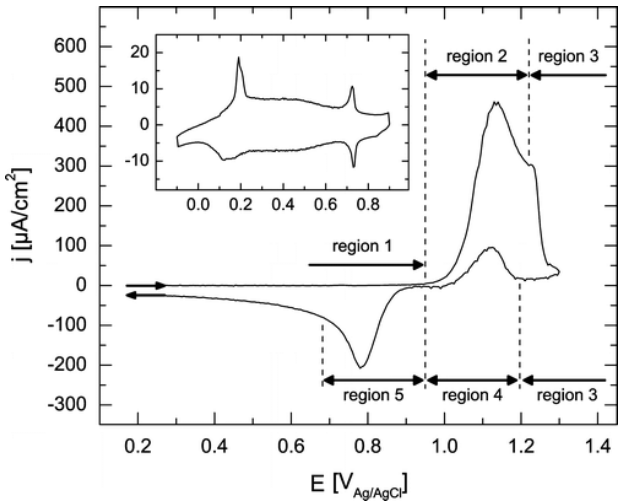

Region 1: double layer regime
Region 2: active dissolution
Region 3: passivation
Region 4: dissolution after passivation
Region 5: redeposition

$$Au + 4Cl^- \leftrightarrow AuCl_4^- + 3e^-$$
$$Au + H_2O \leftrightarrow AuOH + H^+ + e^-$$
$$AuOH \leftrightarrow AuO + H^+ + e^-$$

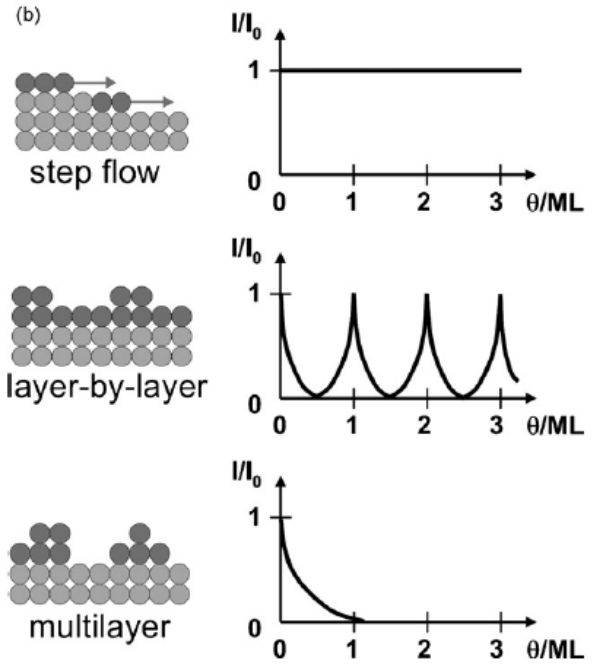

Fig. 3. (a) Reciprocal space geometry for Au(1 0 0), showing Bragg-reflections (filled circles), crystal truncation rods (thick solid lines), reciprocal space positions employed in the measurements (open circles), as well as incoming beam, scattered beam, and momentum transfer q (dashed lines). (b) Schematic curves of the scattered intensity as a function of deposited amount (in monolayers) at anti-Bragg positions for (ideal) step flow, layer-by-layer, and multilayer growth.

Krug et al. J. Phys. Chem. C 114 (2010) 18634.

SXRS – Examples

Au(111) electrochemical dissolution

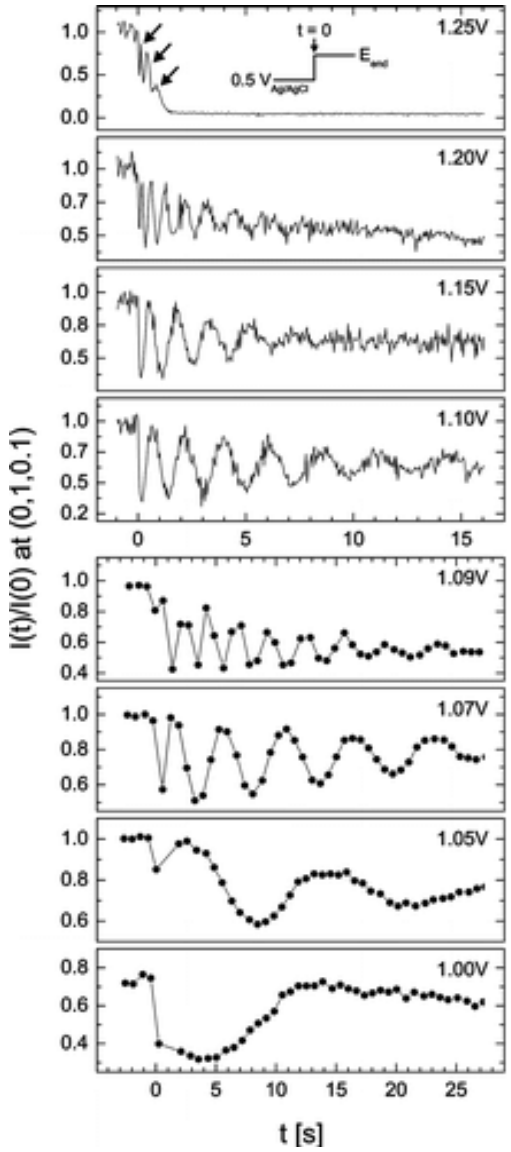

→ oxide formation

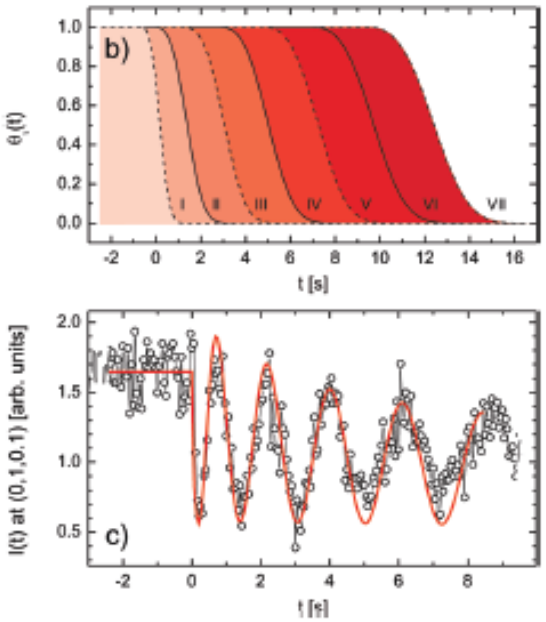

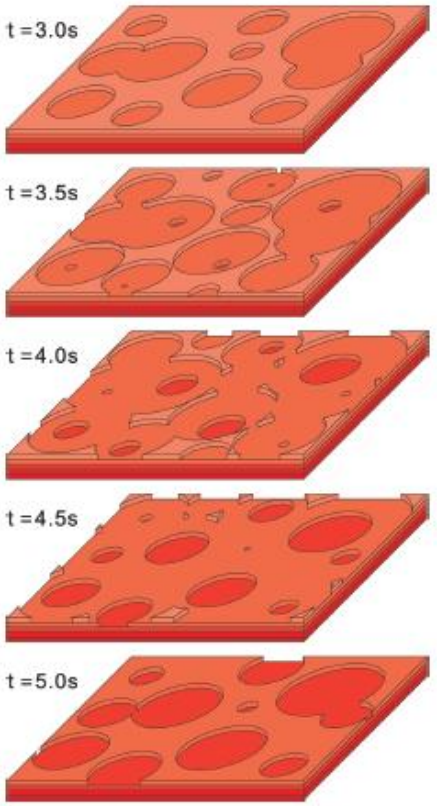

layer-by-layer dissolution

Krug et al. J. Phys. Chem. C 114 (2010) 18634.

Surface X-ray scattering techniques – Basic concepts

Electron density distribution normal to the surface can be derived from Specular Reflectivity data.

Specular Reflectivity $\rightarrow$ Q along (0,0,l)

Ordered water layers:
Vertical ordering: specular rod
Lateral ordering: non-specular rods

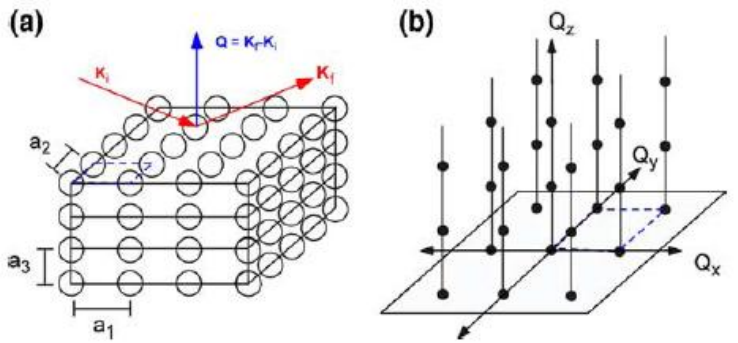

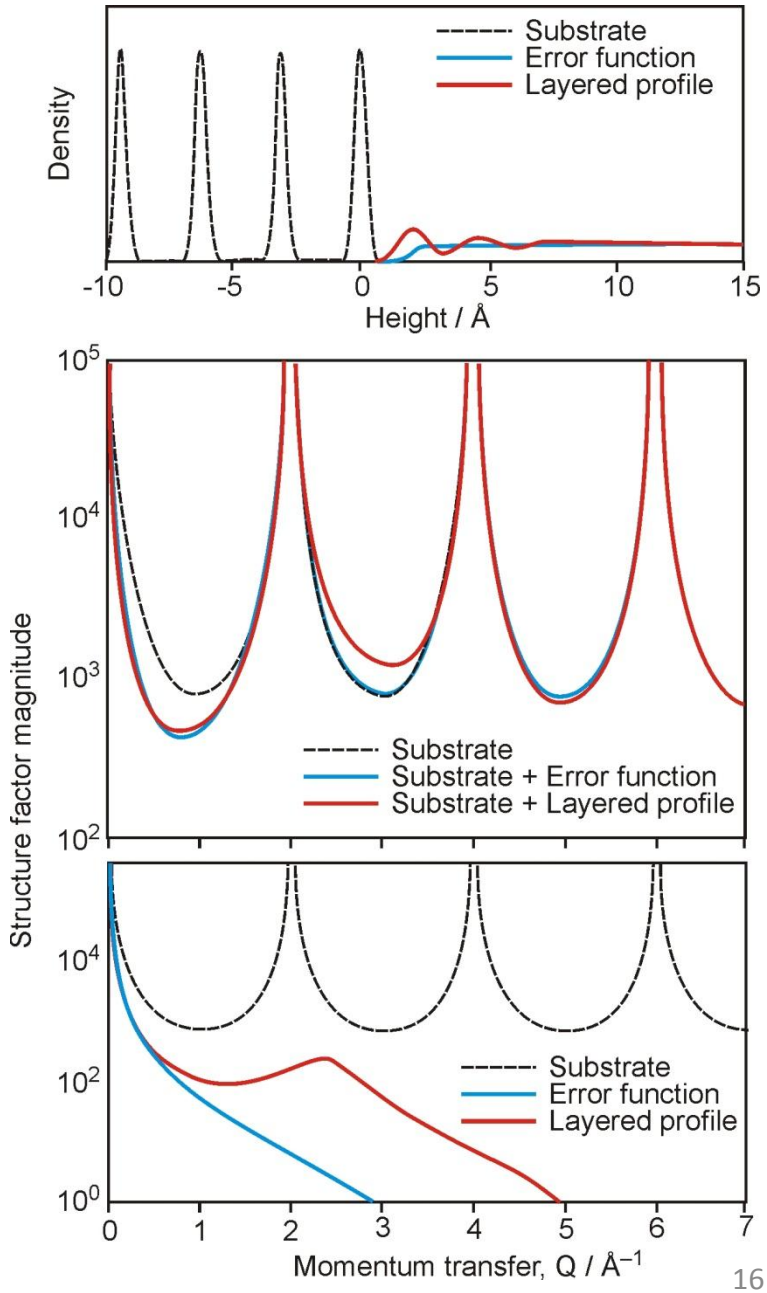

Fenter & Sturchio Prog. Surf. Sci. 77 (2004) 171.

Water on Ag(111)

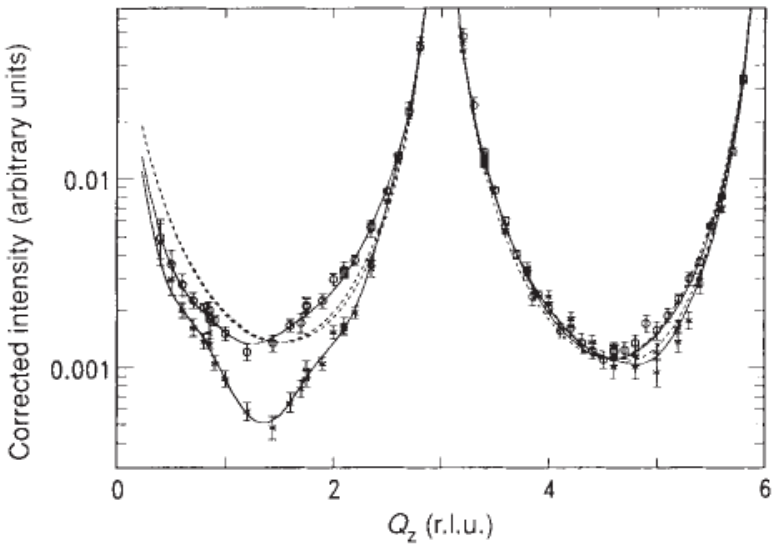

FIG. 3 Integrated intensities of the specular rod for Ag(111) at +0.52 V (stars) and −0.23 V (circles) in 0.1 M NaF, corrected as in Fig. 2. The dashed lines are for bare Ag(111), using the surface roughness and top–second plane spacing obtained from the fits in Fig. 2, but with no contribution from the water distribution. These lines are slightly different at the two voltages, because of the different top–second plane spacings discussed in the text. The solid lines are the best fits with the contribution from the water.

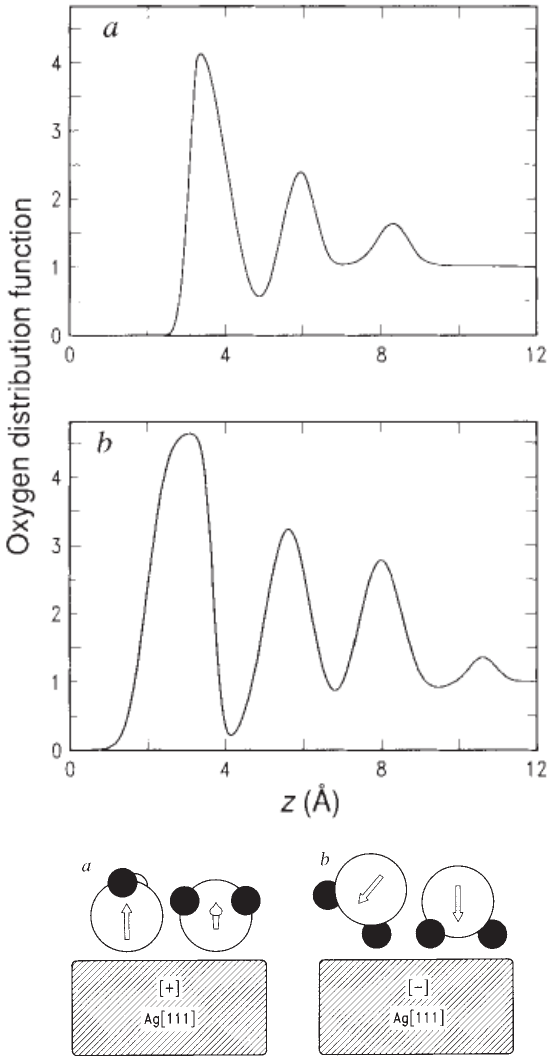

FIG. 1 Possible orientations for water near a surface. *a*, Positively charged surface. *b*, Negatively charged surface. These orientations provide the most favourable electrostatic interactions. The arrows show the directions of the dipole moments. Note that the oxygen atoms are farther from the electrode surface in *b*.

Toney et al. Nature 368 (1994) 444.

Water on mineral surfaces

e.g. rutile TiO_2(110)

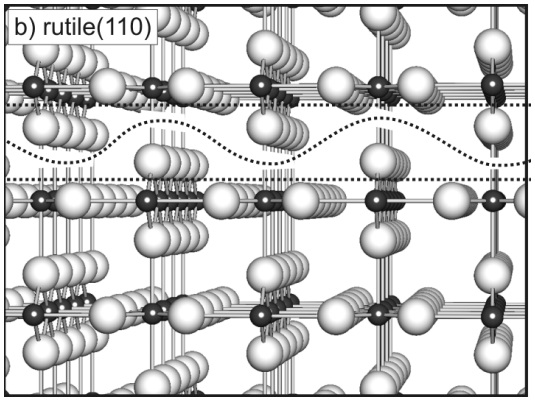

termination in UHV

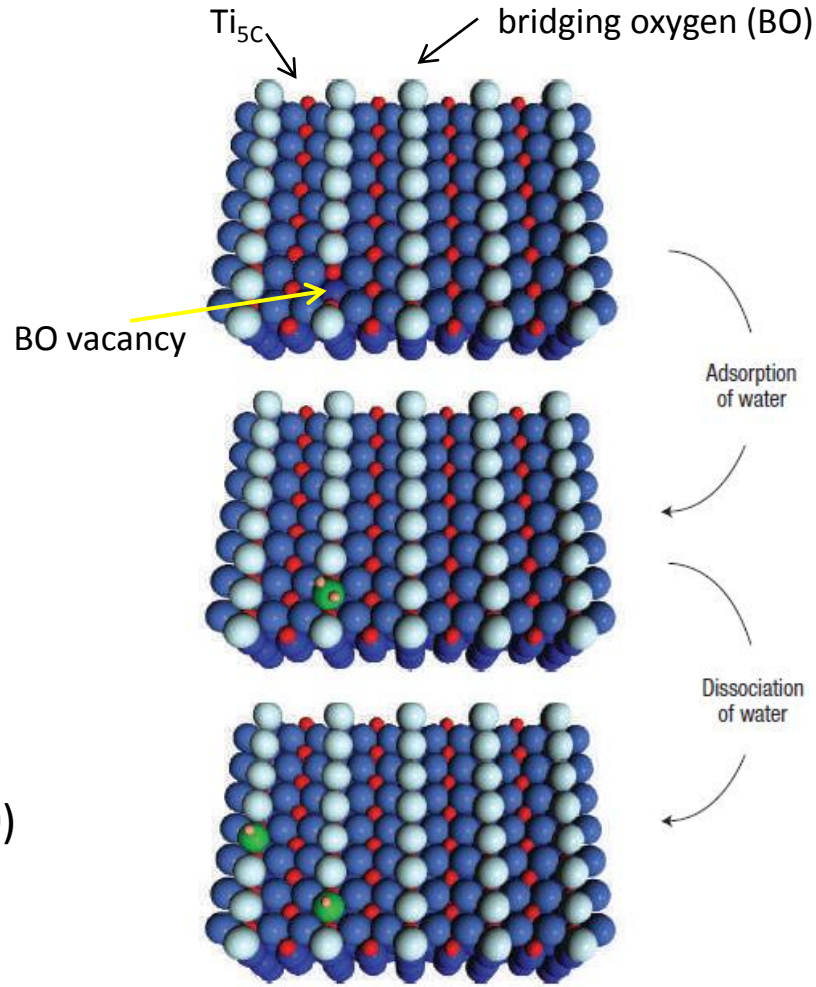

Water chemistry in UHV mediated by bridging oxygen vacancies.

What is the termination of rutile TiO2(110) In water environment?

Bikondoa et al. Nature Mat. 5 (2006) 189.

Water on mineral surfaces

e.g. rutile TiO_2(110)

possible H_2O adsorption sites

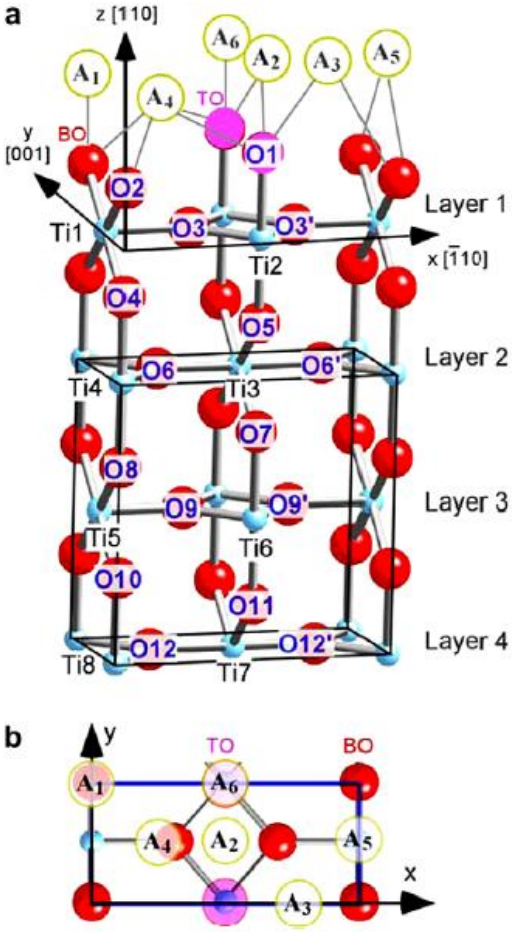

Electron density from CTR

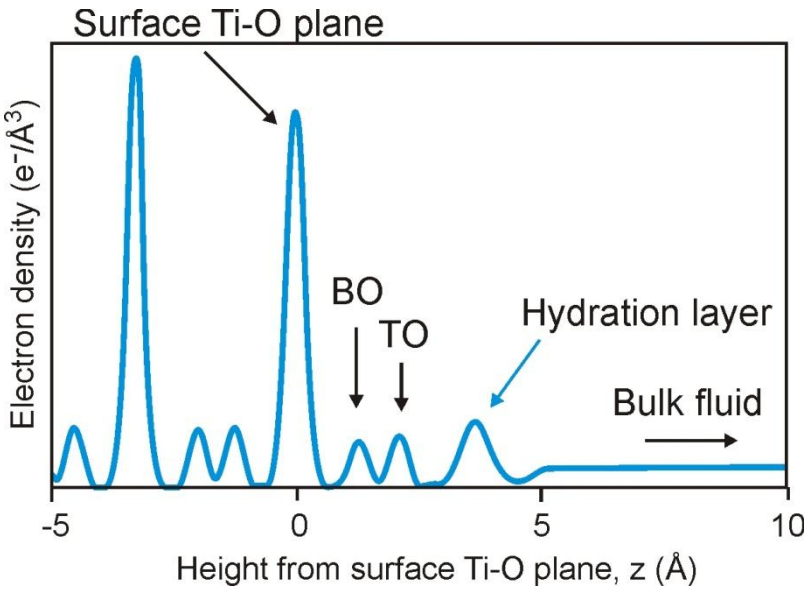

BO: bridging oxygen sites
TO: terminal oxygen sites

A mixture of H_2O and OH^- occupies the TO sites.

Hydration layer consists of three distinct H_2O/unit cell with well-defined vertical and lateral locations.

best fit model

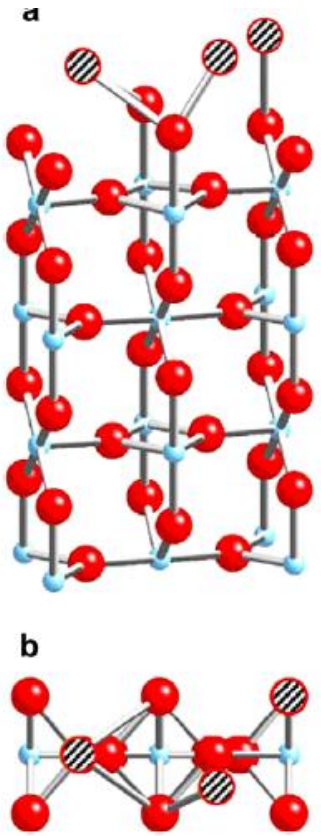

Zhang et al. Surf. Sci. 601 (2007) 1129.

Resonant Anomalous X-Ray Reflectivity

Resonant anomalous x-ray reflectivity (RAXR) makes use of the 'anomolous' dispersion in the atomic scattering factor of an atom near its characteristic absorption edge. This allows for the possibility of incorporating element-specific information into the x-ray scattering methods. Both the real (f') and imaginary (f'') parts of the scattering factor are modified which are related to each other by Kramers-Kronig relations. The imaginary part of the resonant scattering factor, f''(E) is proportional to the x-ray absorption near edge structure (XANES) profile that could be measured in x-ray absorption spectroscopy. Consequently RAXR brings together the unprecedented structural sensitivity and interfacial specificity of x-ray reflectivity measurements with the element-specificity and spectroscopic sensitivity of XANES measurements leading to a much more complete understanding of the complex structural and chemical changes of many important interfacial processes.

Resonant atomic scattering factor:

$$f(q_0, E) = f_{NR}{}^0(q_0) + f_R{}'(E) + i f_R{}''(E)$$

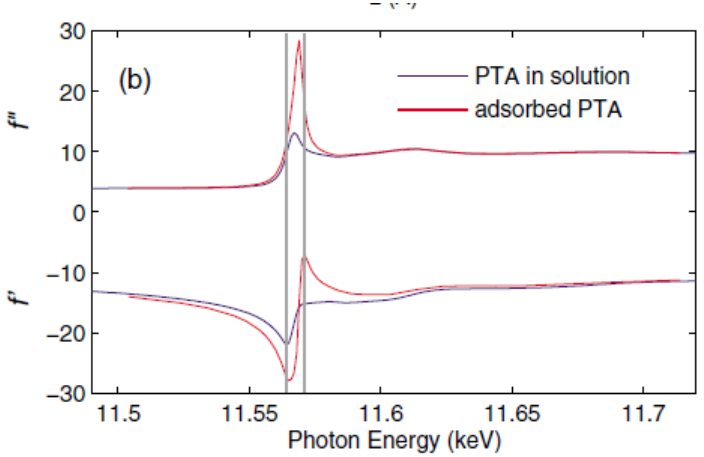

http://www.cse.anl.gov/Nuclear_and_Environmental_Processes/RAXR.shtml

An example from catalysis – Catalyst preparation

Impregnation of silica with PTA, $Pt(NH_3)_4(OH)_2$ – electrostatic adsorption or inner sphere complex?

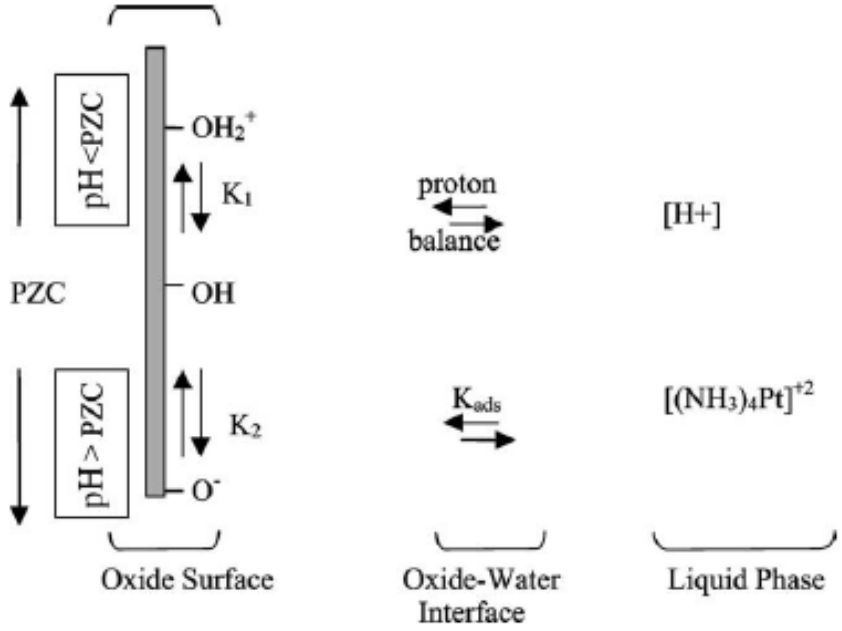

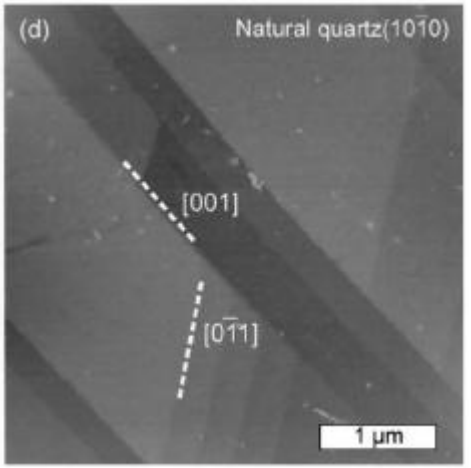

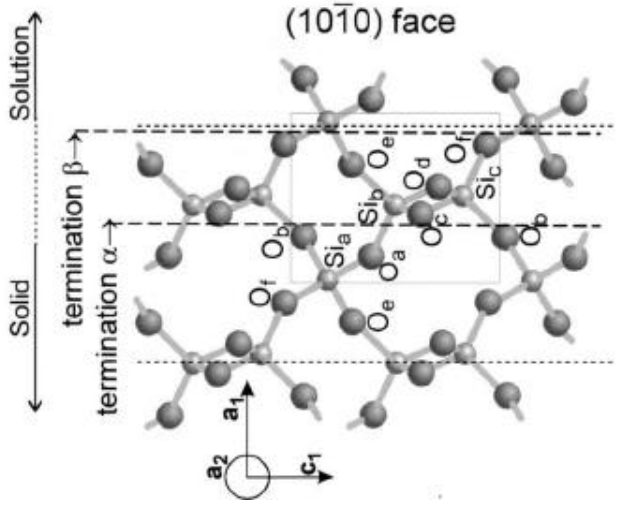

$$2(\mathrm{Si{-}O^-, H^+}) + \left[\mathrm{Pt(NH_4)_3}\right]^{+2}, (\mathrm{OH^-})_2 \longleftrightarrow (\mathrm{Si{-}O^-})_2, \left[\mathrm{Pt(NH_4)_3}\right]^{+2} + 2(\mathrm{H^+}, \mathrm{OH^-}).$$

Schlegel et al. Geochim. Cosmochim. Acta 66 (2002) 3037.

An example from catalysis – Catalyst preparation

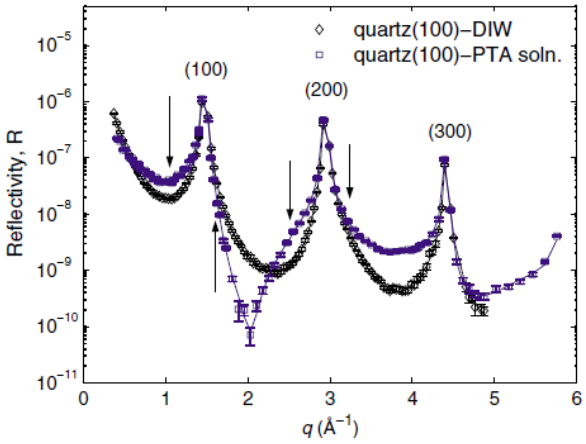

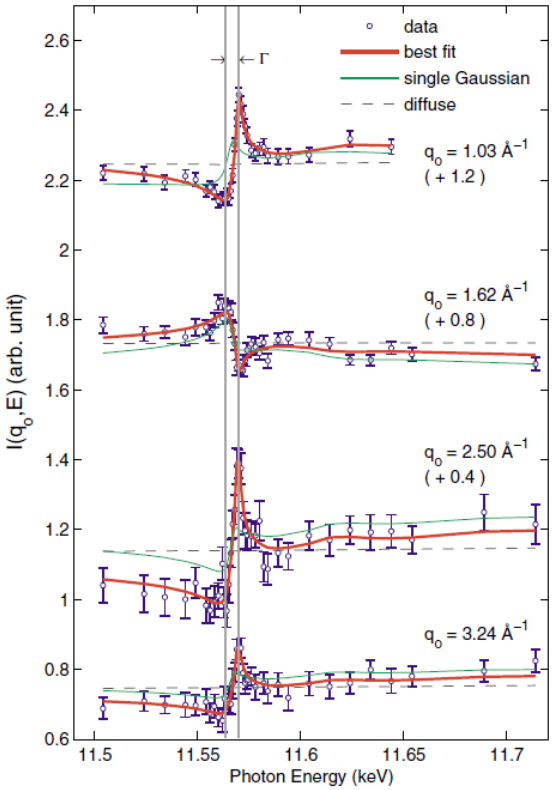

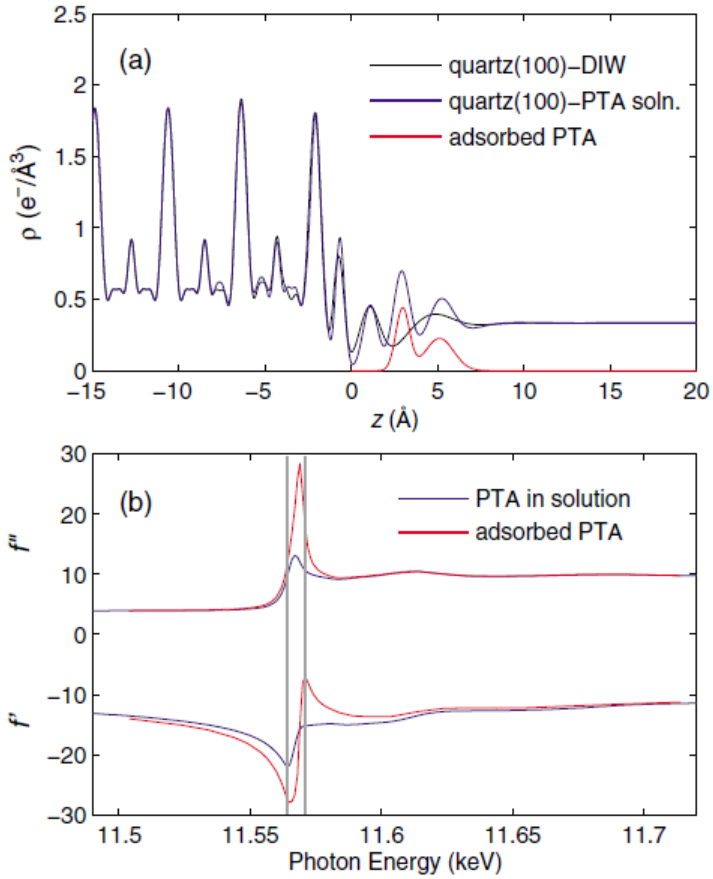

outer sphere PTA complexes at z = 3 Å and 5 Å

inner sphere complex (specific adsorption) would be located in the surface hydration layer at z = 1 Å.

Park et al. Phys. Rev. Lett. 94 (2005) 076104.

CO adsorption and oxidation on Pt(111)

$CO_{ad} + OH_{ad} \rightarrow CO_2 + H^+ + e^-$

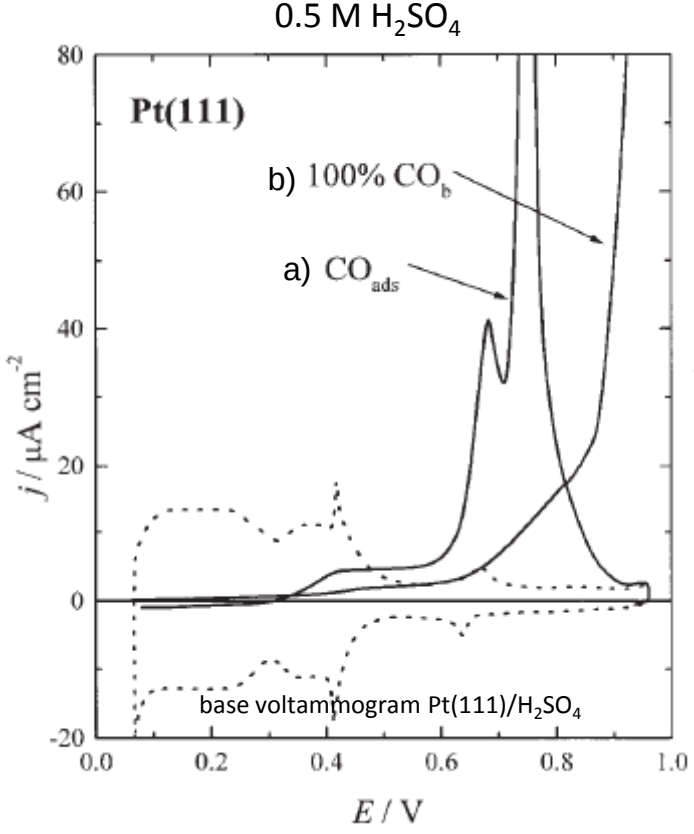

a) CO stripping (only chemisorbed CO)
b) CO oxidation (CO-saturated electrolyte)

Searching for long-range ordered structures of CO on Pt(111).
→ super structure truncation rods

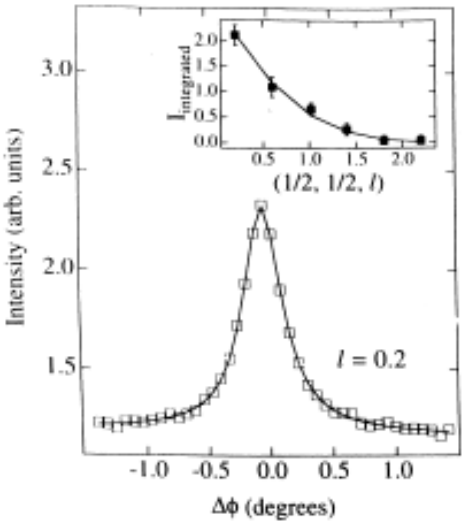

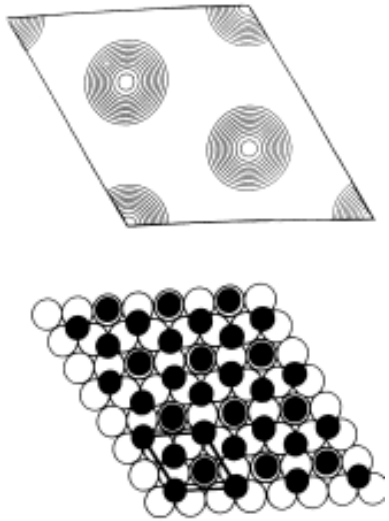

⇒ ordered p(2×2)-3CO adsorbed layer

Lucas et al. Surf. Sci. 425 (1999) L381.

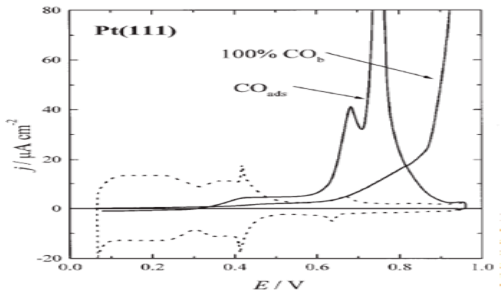

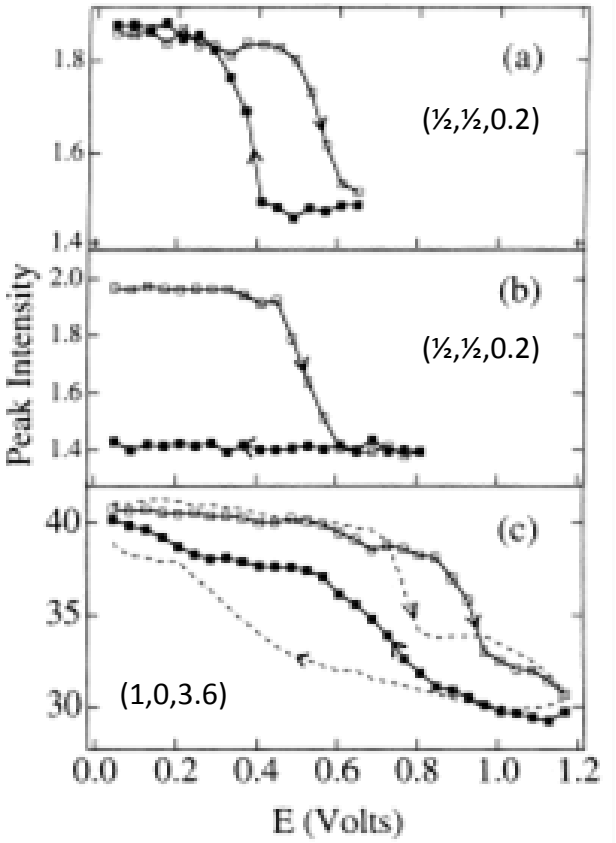

a) CO oxidation (CO-saturated electrolyte)
b) CO stripping (only chemisorbed CO)
c) lattice expansion caused by CO adsorption

↘ outward relaxation of first Pt layer

Lucas et al. Surf. Sci. 425 (1999) L381.

(½ , ½ ,l) rod disappears before complete CO desorption
→ disordered CO adlayer or another ordered structure?

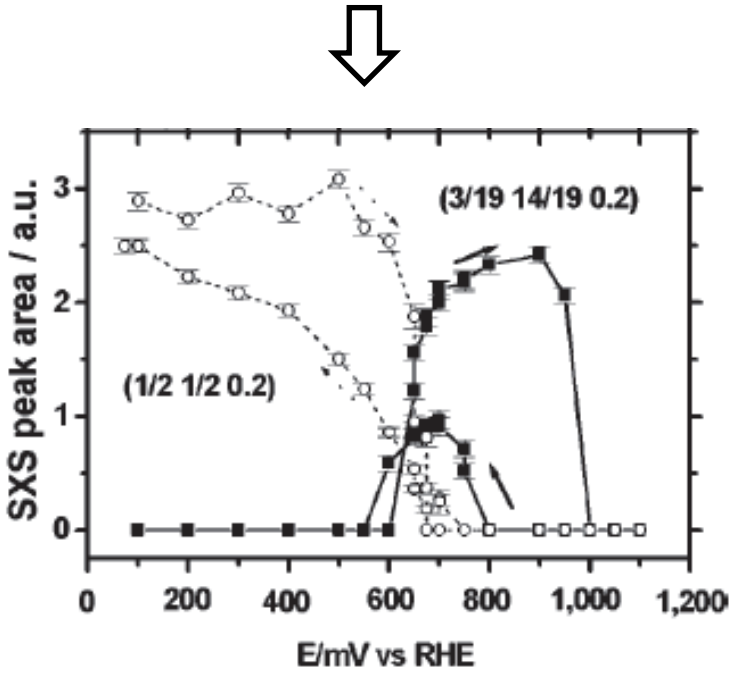

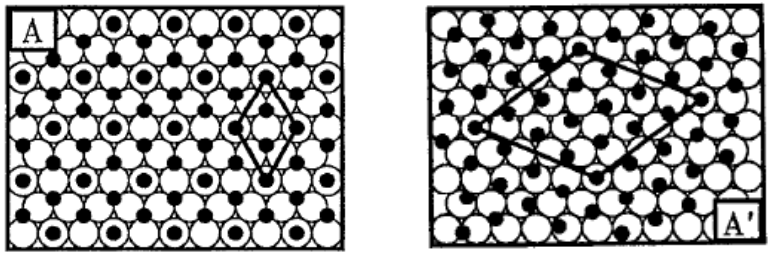

p(2×2)-3CO → (√19×√19)-13CO

Tolmachev et al. Electrochem. Sol. State Lett. 7 (2004) E23.

Principle of Scanning Tunneling Microscopy

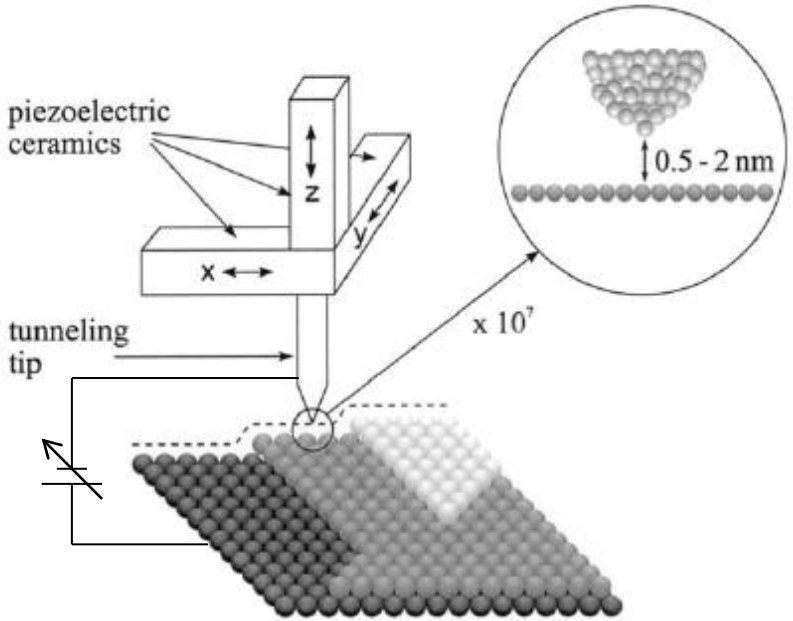

Tunneling

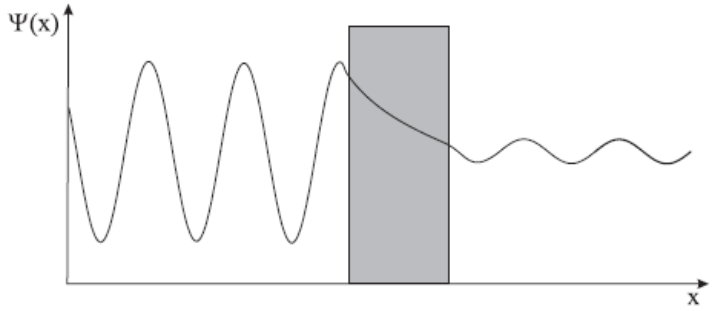

STM tunneling junction

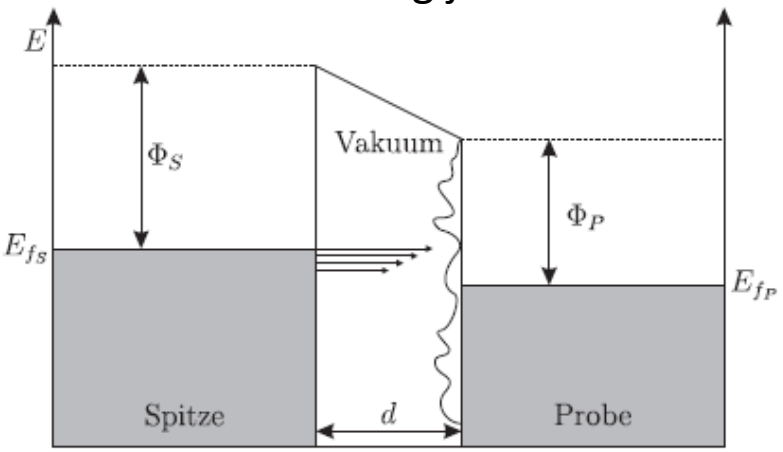

constant current mode

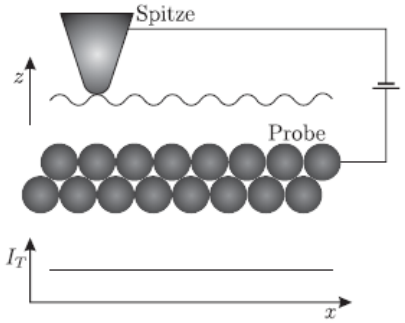

image from C. Schlaup, PhD Thesis, Bonn, 2010.

Electrochemical Scanning Tunneling Microscopy

Features of STM in electrolyte solution

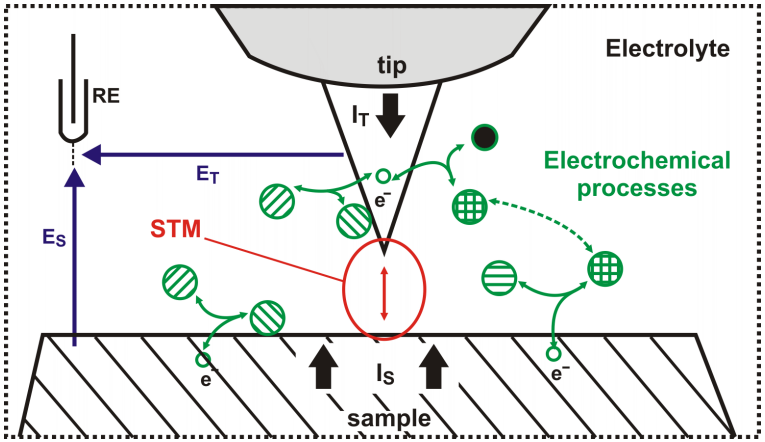

Potentiostatic STM

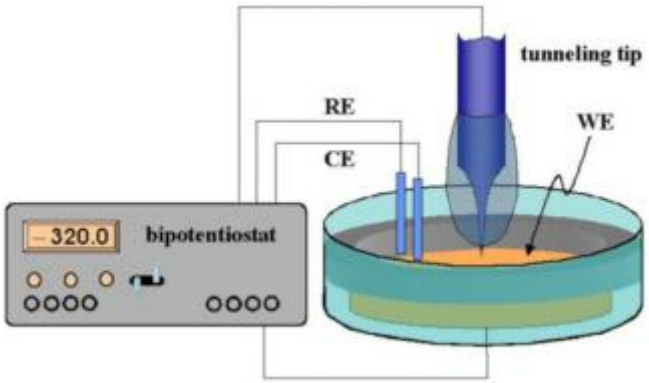

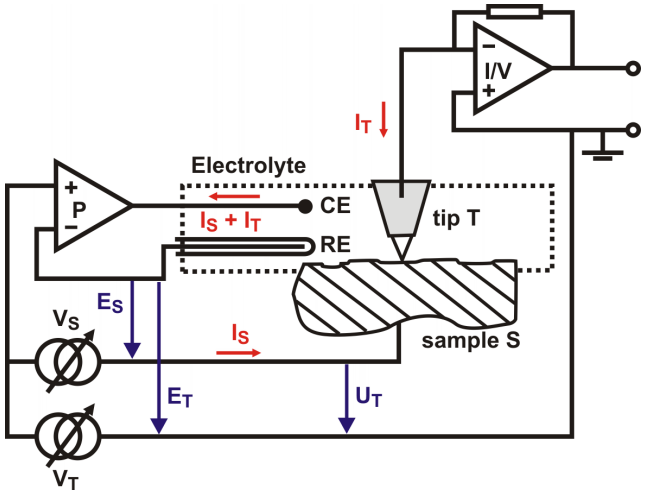

Important:
Diminution of unwanted electrochemical reactions at the tip.
Control of electrochemical processes at the electrode during and between STM imaging.

H. Siegenthaler, in: Scanning Tunneling Microscopy II; R. Wiesendanger, H.-J. Güntherodt (Eds.) Springer Series in Surface Sciences 28.

Electrochemical Scanning Tunneling Microscopy

Tip coating is necessary to avoid electrochemical reactions at the tip

uncoated Pt/Ir tip

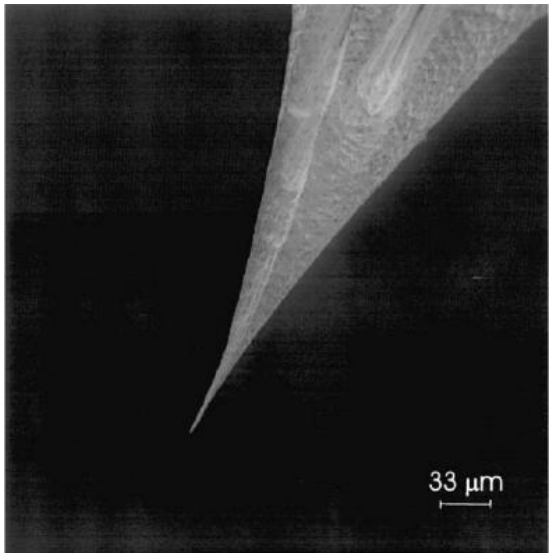

D. Mayer et al. *J. Electroanal. Chem.* 524 (2002) 20.

coated tip, only tip apex is uncoated

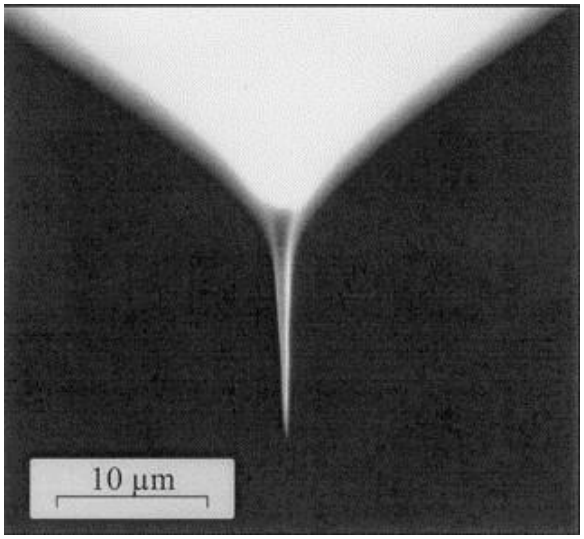

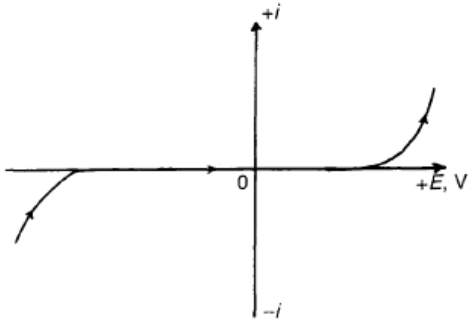

Figure 7 Typical electrochemical response of an STM tip. The Faradaic current flowing in the cathodic region is due to H_2 evolution and the anodic current is due to O_2 evolution or tip dissolution.

EC-STM

Example: potential-dependent surface structure in electrolyte solution
Au(111) in 0.05 M H_2SO_4.

I: Au(111) (23x√3) reconstruction
(compressed first layer)
II: lifting of reconstruction
(Au ad-islands)
III: ordered sulfate layer

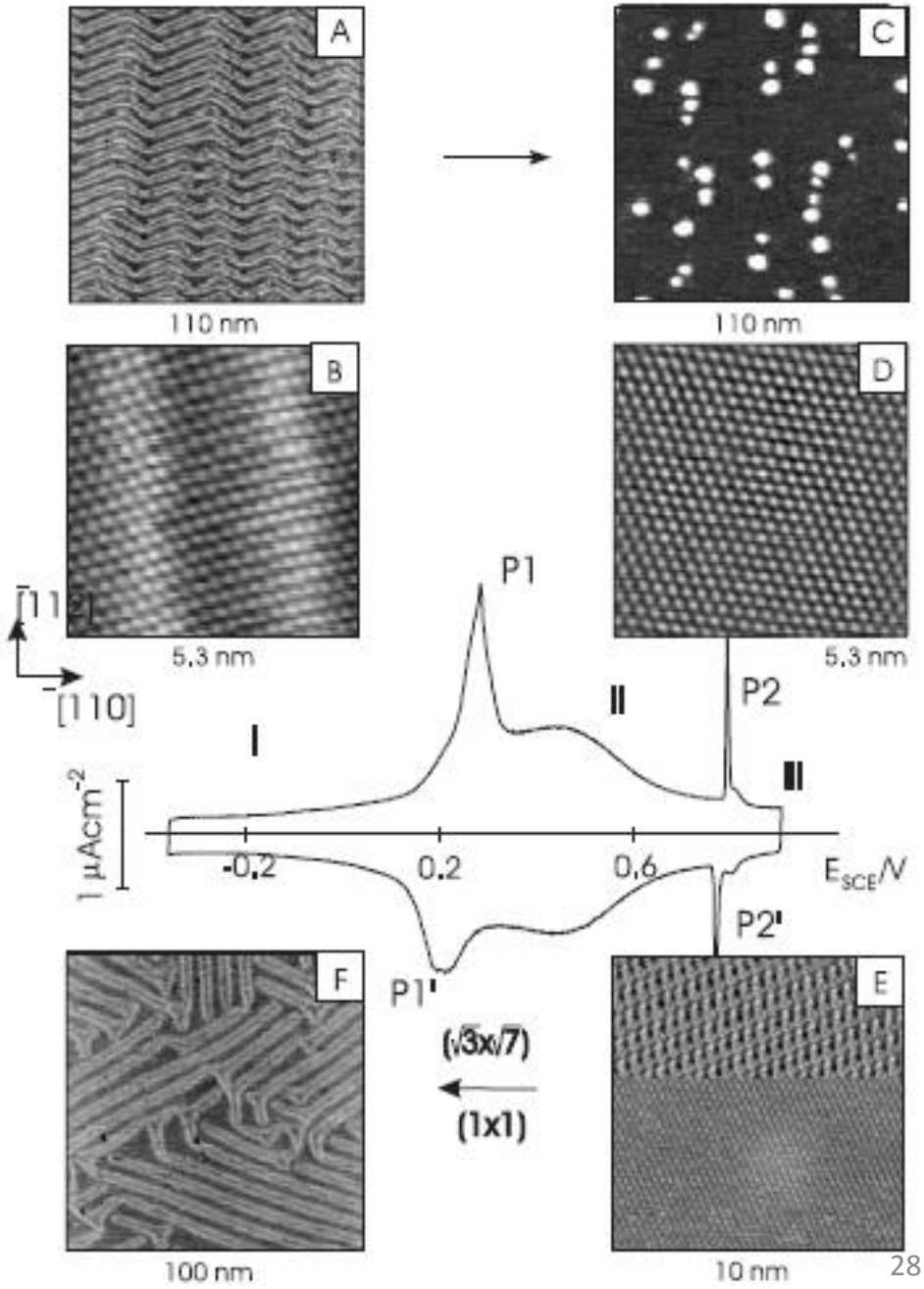

Dretschkow, Wandlowski, in Wandelt, Thurgate (Eds.) *Topics Appl. Phys.* 85 (2003) 259.

EC-STM

Anion adsorption
e.g. $PdCl_4^{2-}$ on Au(100)

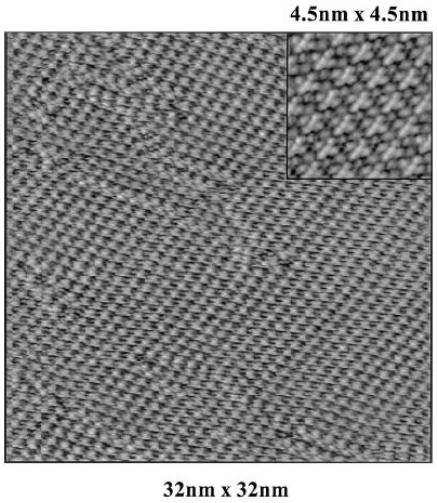

upd: under potential deposition
formation of a metal monolayer on a foreign substrate at potentials positive of the corresponding Nernst potential

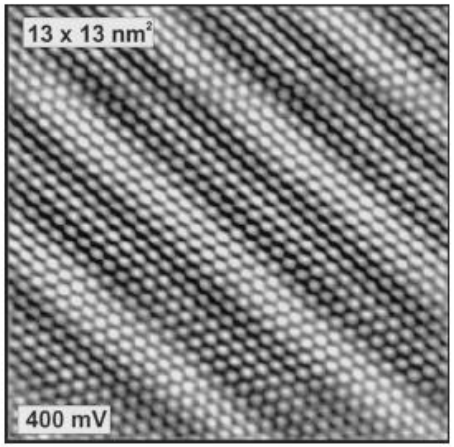

Au(111): Onset of oxidation

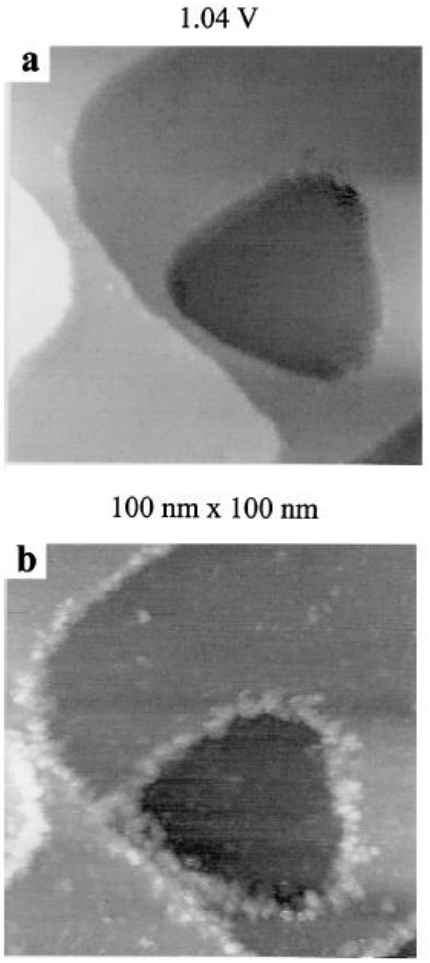

Fig. 9. STM images of Au(111) in 0.1 M H_2SO_4, showing the onset of oxidation at the steps. (a) At 1.04 V versus SCE step edges are clear; (b) at 1.15 V versus SCE step edges are decorated with oxide. From reference [111].

"Nanostructuring"
Cu clusters on Au(111)

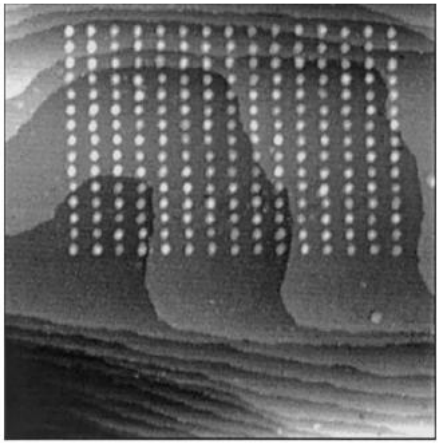

SAM: self assembled monolayers
Alkanethiols on Au(111)

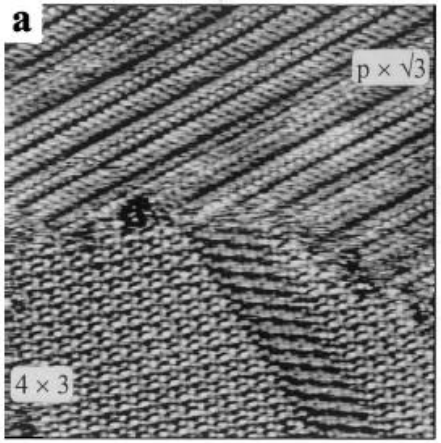

All images from:
D. Kolb, Electrochim. Acta 45 (2000) 2387.

EC-STM

Potential-tuned resonant tunneling through redox molecules

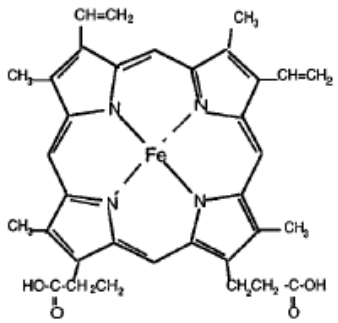

1. Fe-Protoporphyrin IX

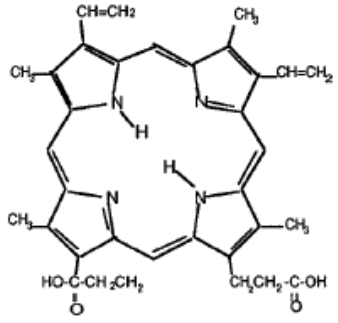

2. Protoporphyrin IX

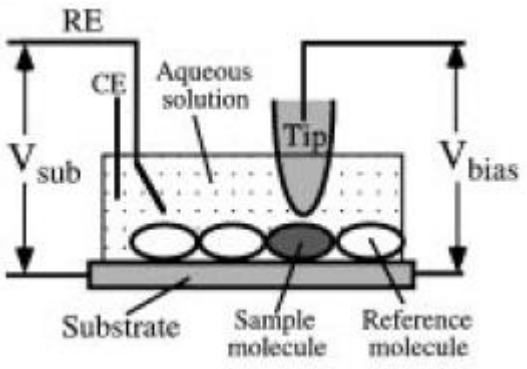

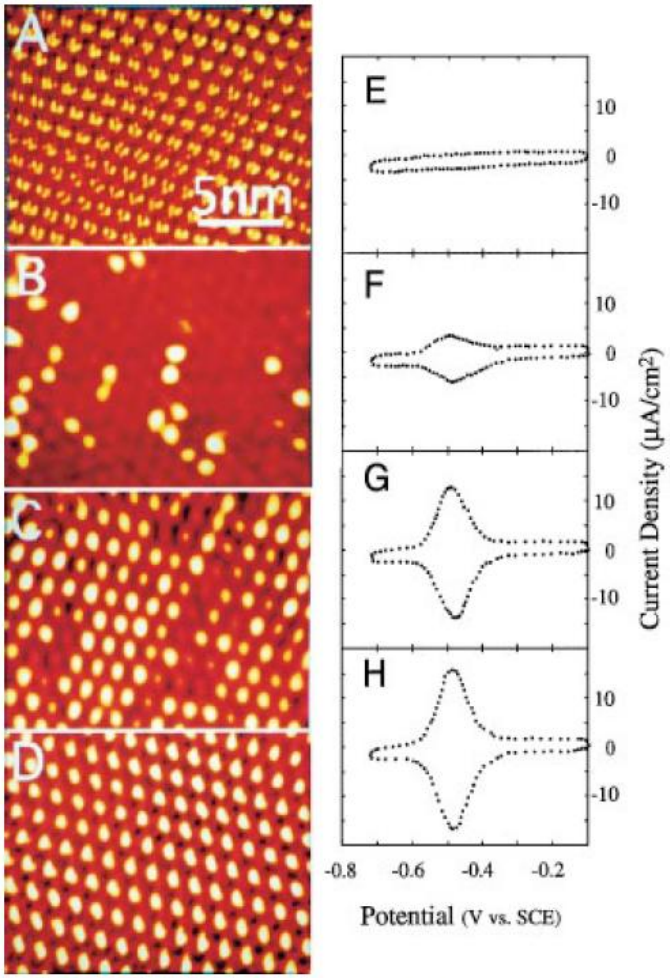

FIG. 3 (color). STM images of FePP/PP adsorbed on a graphite substrate from 0.05*M* $Na_2B_4O_7$ solutions containing FePP and PP at the ratio of 0:1 (A), 1:4 (B), 4:1 (C), and 1:0 (D). The images were taken with a substrate potential of −0.41 V, a tunneling current of 30 pA, and a tip-substrate bias of −0.1 V. High frequency noise has been removed from the images. (E)–(H) are the corresponding cyclic voltammograms obtained with a sweeping rate of 0.2 V/sec.

N.J. Tao, Phys. Rev. Lett. 76 (1996) 4066.

EC-STM

Potential-tuned resonant tunneling through redox molecules

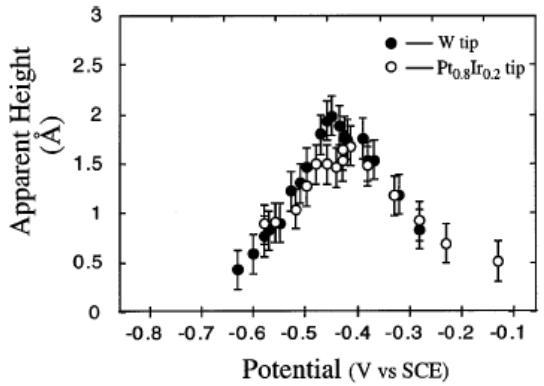

FIG. 5. Apparent height of FePP relative to PP as a function of the substrate potential. The data obtained with the $Pt_{0.8}$-$Ir_{0.2}$ tip and with the W tip are represented by open circles and filled circles, respectively.

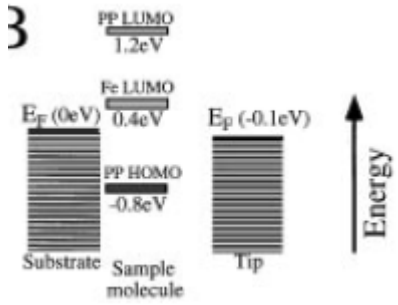

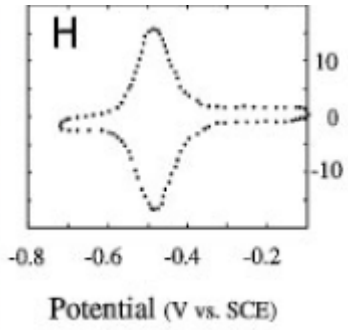

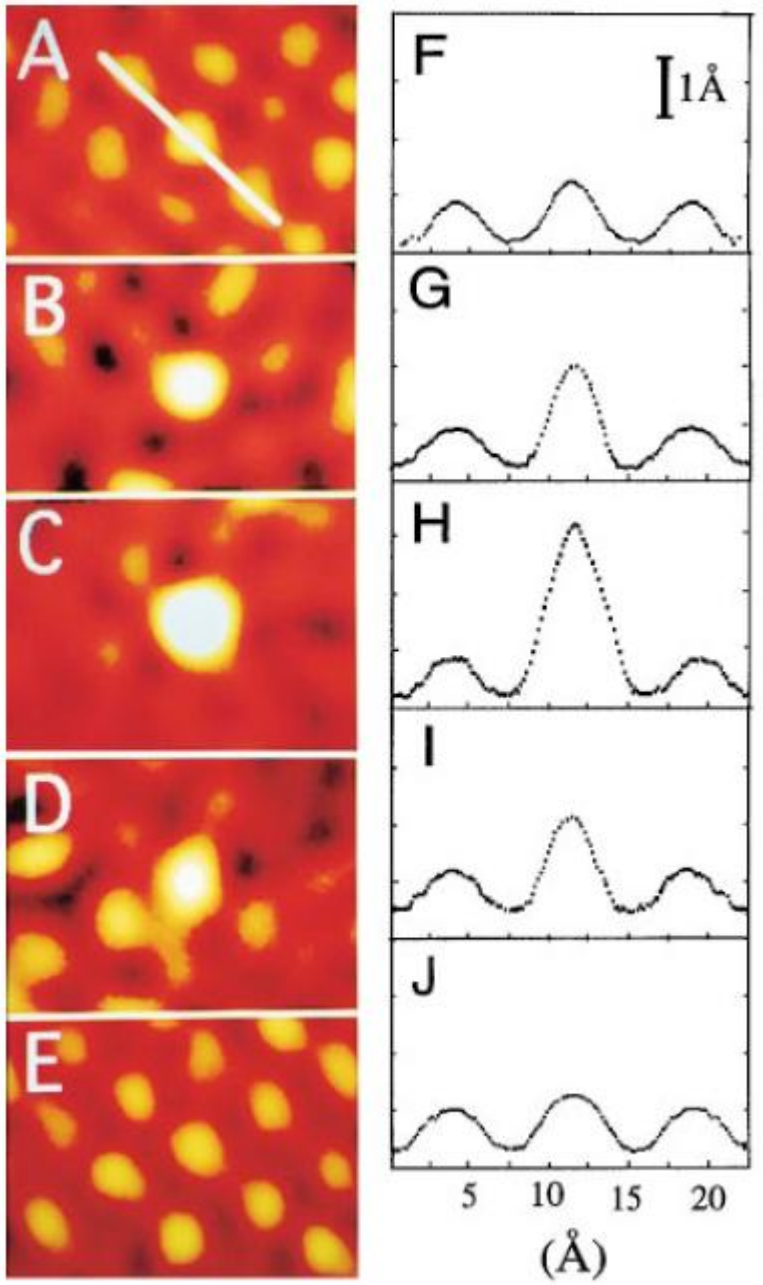

FIG. 4 (color). STM image of an FePP molecule embedded in an ordered array of PP molecules when the substrate was held at −0.15 (A), −0.30 (B), −0.42 (C), −0.55 (D), and −0.65 V (E), respectively. (F)–(J) are the corresponding plots of the cross sections along the white line indicated in (A). The data were symmetrized with respect to the center.

N.J. Tao, Phys. Rev. Lett. 76 (1996) 4066.

EC-STM

Potential-pulse pertubation

TPyP porphyrin

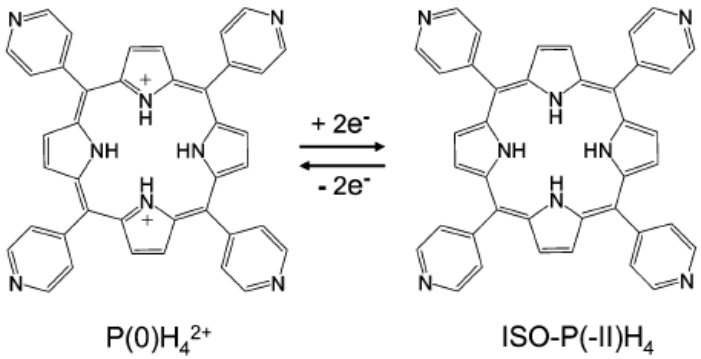

Figure 1. Experimental method: potential-pulse perturbation. SCE = saturated calomel electrode.

A-E: increasing oxidation pulse duration
E-F: same area (after 3 min.)

redistribution of ox. TPyP molecules (images E and F) suggests surface charge diffusion, i.e. electron transfer between TPyP molecules.

bright: reduced TPyP
dark: oxidized TPyP

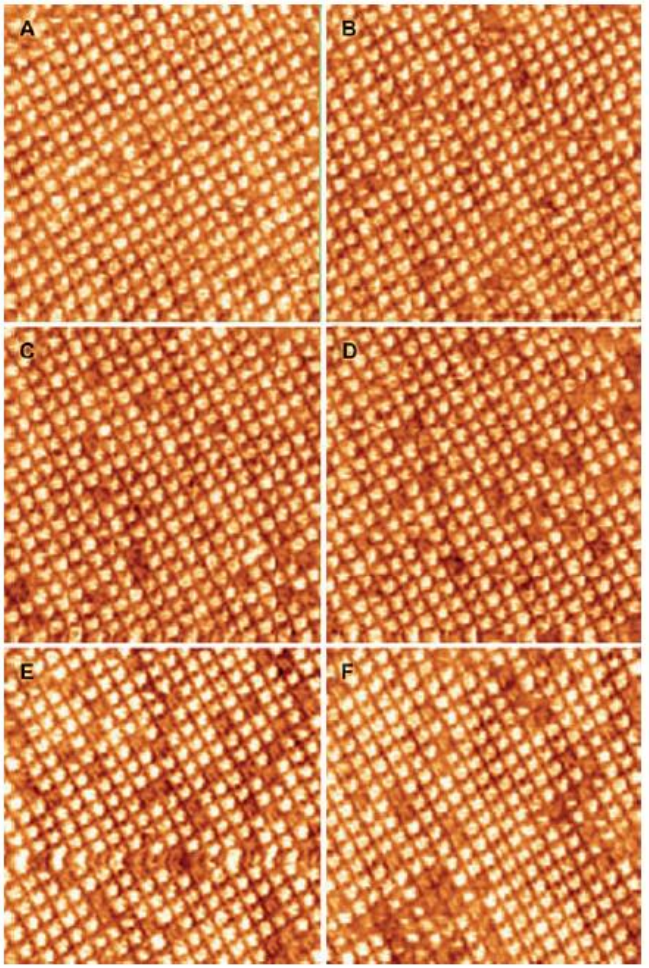

Figure 2. Pre-adsorbed TPyP/Au(111) in 0.1 M H_2SO_4 at a potential of −0.1 V_{SCE} (27×27 nm^2). A) Before the oxidation potential pulse was applied, and after oxidation of adsorbed TPyP molecules with a potential pulse of 0.2 V for duration: B) 0.1 s, C) 0.2 s, D) 0.5 s, E) 1 s. F) STM image at −0.1 V 3 min after obtaining image (E). Dark spots are oxidized TPyP molecules, light spots are reduced TPyP molecules.

He & Borguet, Angew. Chem. Int. Ed. 46 (2007) 6098.

STM in organic solvent

Mn porphyrin as oxidation catalyst
for transformation of alkenes into epoxides

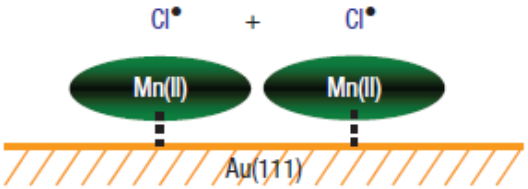

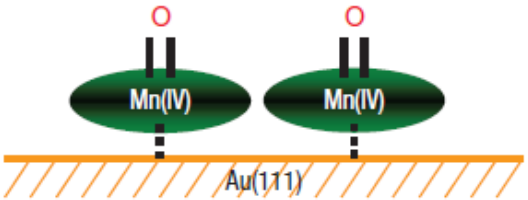

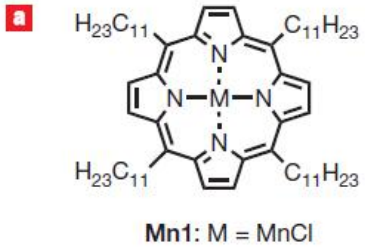

Mn1: M = MnCl

oxygen free

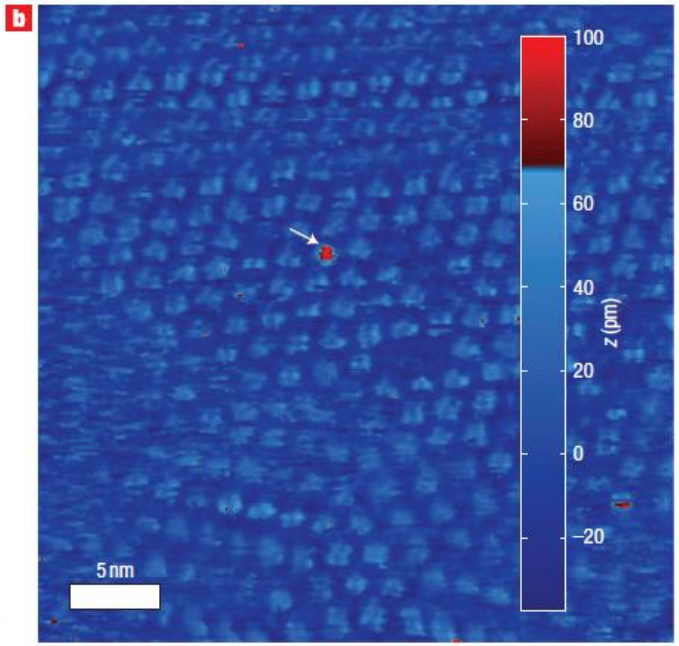

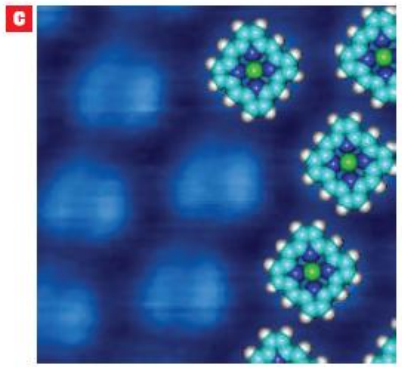

+ O_2

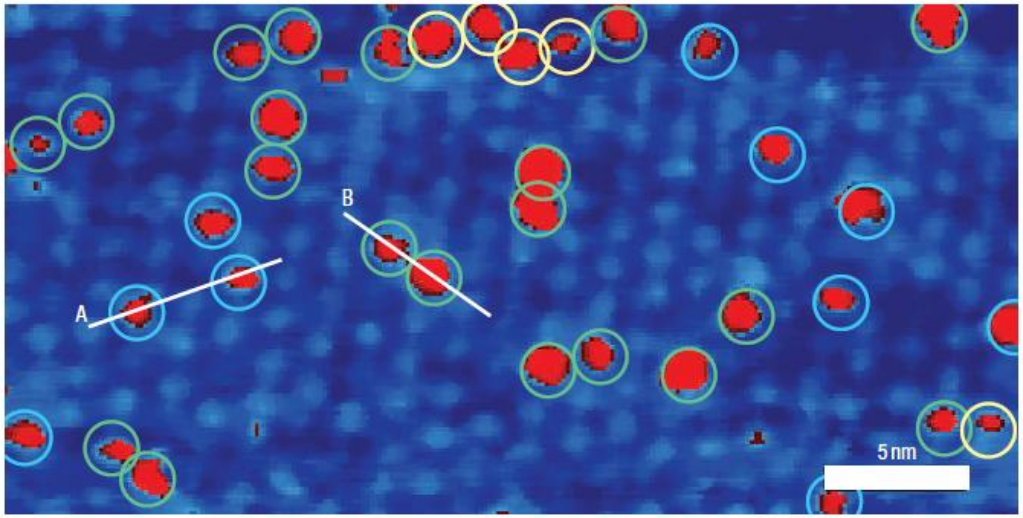

Hulsken et al. *Nature Nanotechnolgoy* 2 (2007) 285.

STM in organic solvent

Mn porphyrin as oxidation catalyst
for transformation of alkenes into epoxides

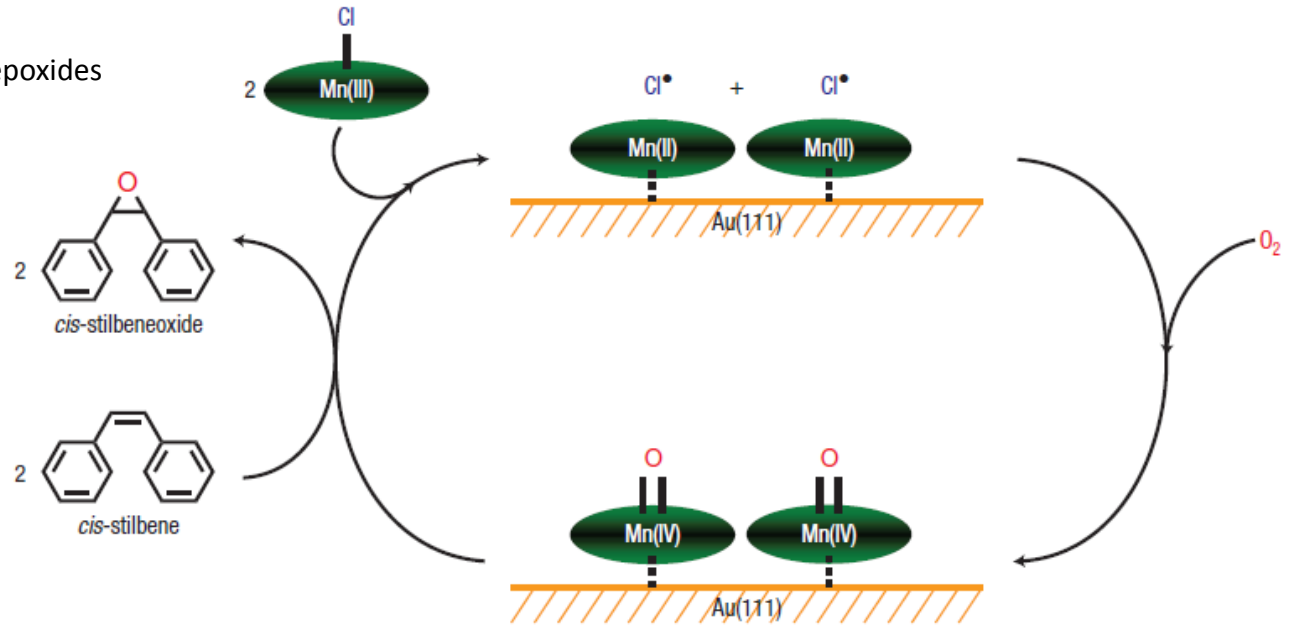

+O_2 ⇒ +stilbene ⇒

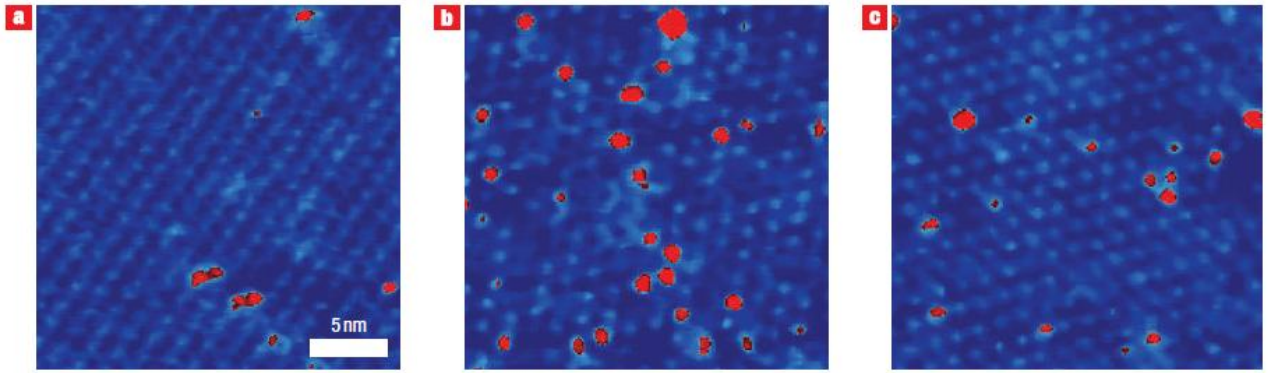

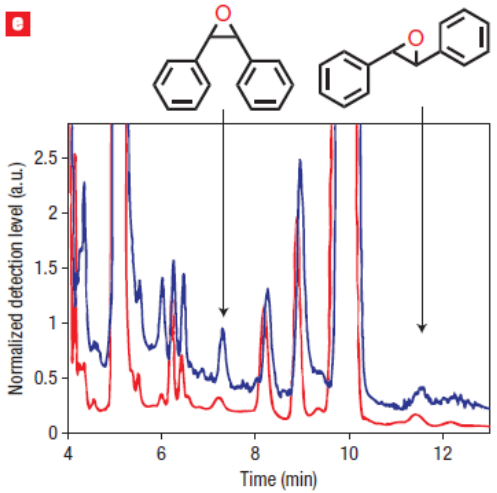

Hulsken et al. *Nature Nanotechnolgoy* 2 (2007) 285.

EC-STM

Electrochemically induced 2D Polymerization in the liquid STM.

Polyaniline (PAn) $x C_6H_5\text{-}NH_2 \rightarrow -(C_6H_4\text{-}NH)_x- + 2xH^+ + 2xe^-$

Au(111), 0.1 M H_2SO_4+30 mM aniline

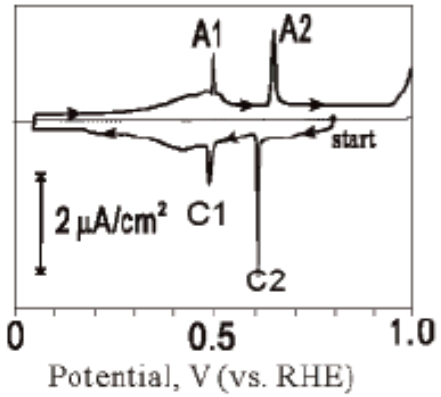

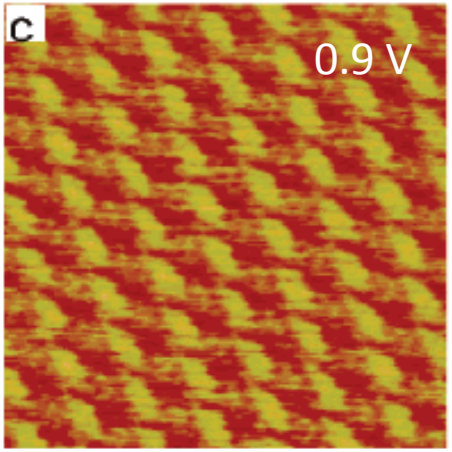

7 nm x 7 nm

Polymerization start: formation of a diradical cation at positive potential

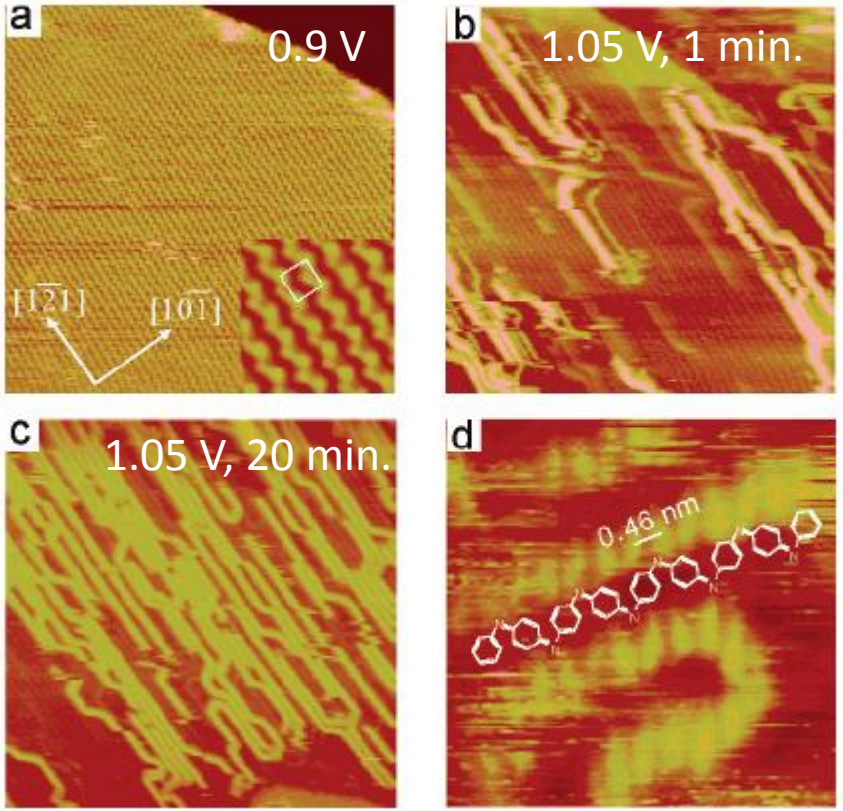

50 nm x 50 nm

6 nm x 6 nm

Yang et al. *J. Am. Chem. Soc.* 129 (2007) 8076.

Scanning Electrochemical Microscopy – SECM

The probing feedback quantity is a faradaic current flowing at an ultramicroelectrode probe in µm-scale distance from the sample.

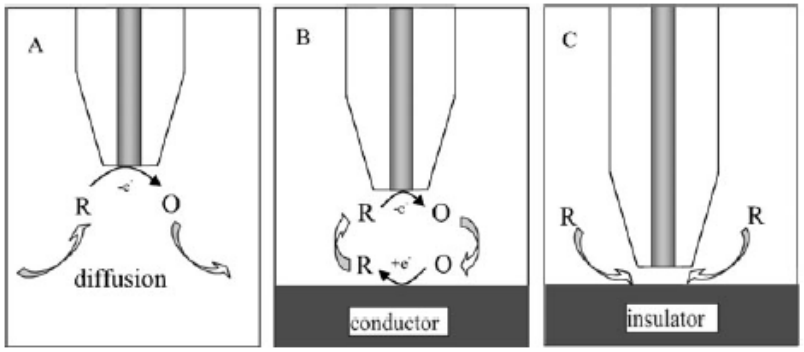

Fig. 3 Feedback mode of the SECM operation. (A) The UME tip is far from the substrate. (B) Positive feedback: species R is regenerated at the substrate. (C) Negative feedback: diffusion of R to the tip is hindered by the substrate.

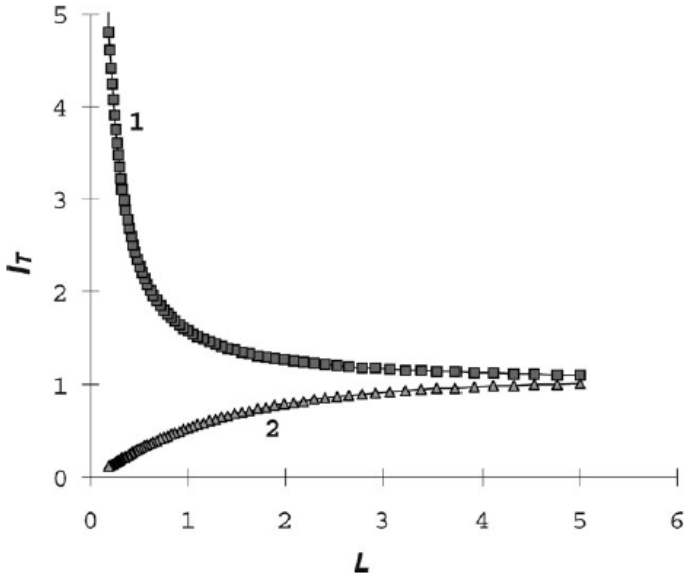

Fig. 6 Theoretical approach curves for a tip electrode over a conductive (1) and insulating (2) substrate. Solid lines are computed for RG = 10 from eqn (7) (curve 1) and eqn (8) (curve 2). Symbols are from simulations in ref. 7.

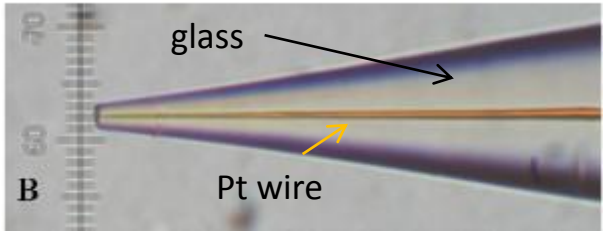

www.electrochem.cwru.edu/encycl

Sun et al. PCCP 9 (2007) 802.

Scanning Electrochemical Microscopy – SECM

Example: Oxygen reduction reaction

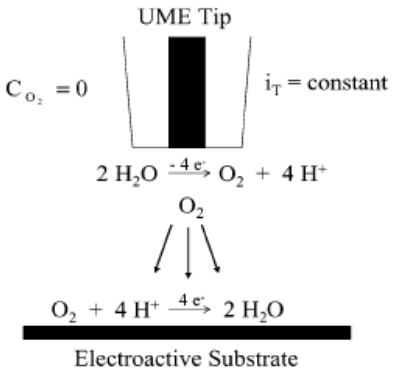

a) Screening of catalysts: Pd-Au-Co ternary alloys

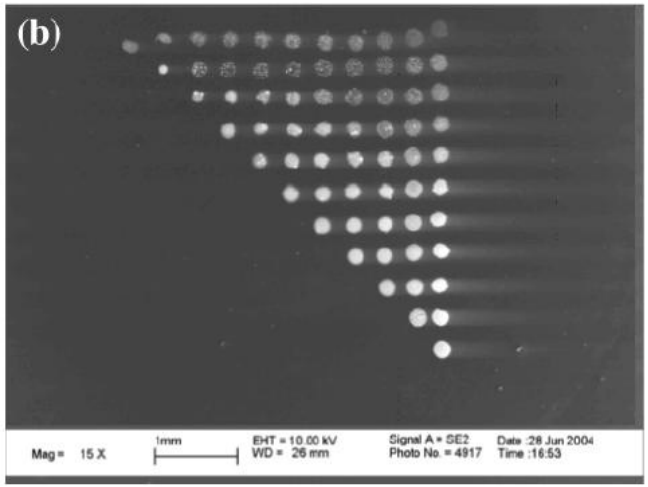

Figure 4. SEM images of typical binary (a) and ternary (b) catalyst arrays. (a) Pd–Co; (b) Pd–Au–Co.

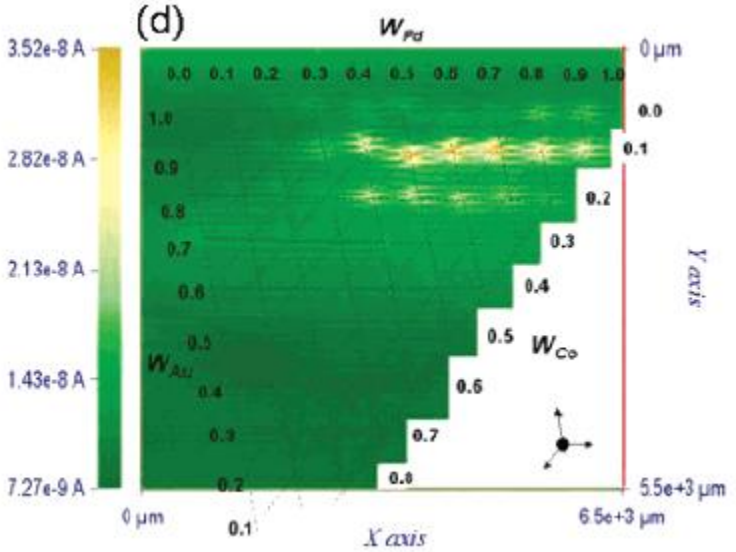

Fernandez et al., J. Am. Chem. Soc. 127 (2005) 357.

b) Structure-sensitive catalysis: shape-controlled Pt nanoparticles

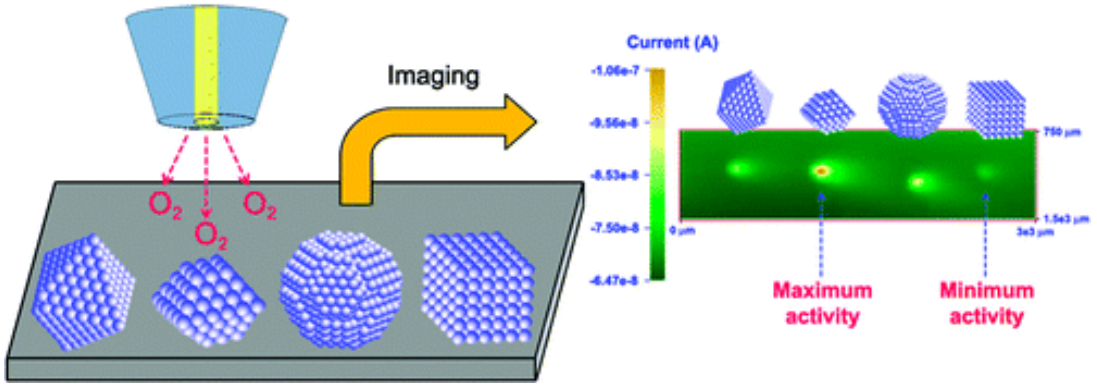

Sanchez-Sanchez et al., J. Am. Chem. Soc. 132 (2010) 5622.

Scanning Force Microscopy – SFM (AFM)

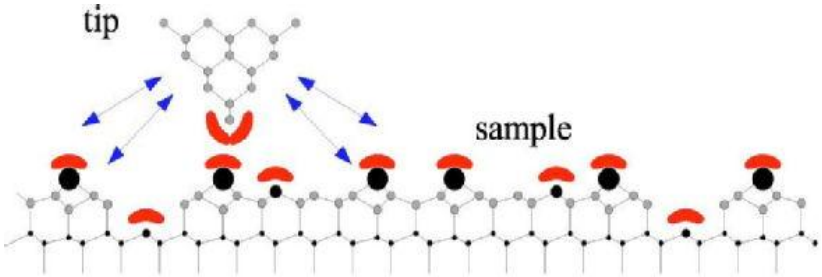

Attractive forces:
- van der Waals
- electrostatic
- chemical

Repulsive forces:
- hard sphere repulsion
- Pauli exclusion interaction
- electron electron Coulomb interaction

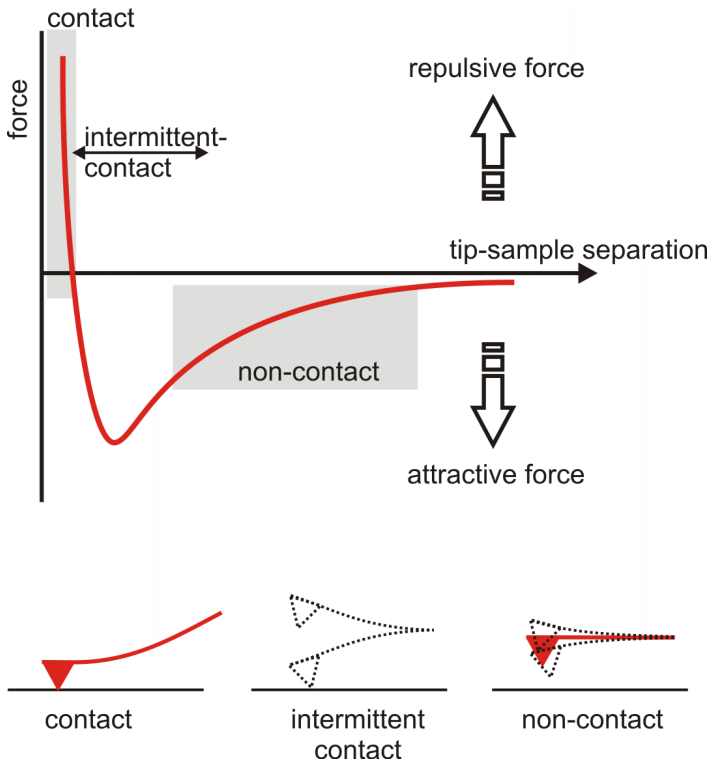

In electrochemical environment similar to STM
In addition: insulators, biological samples

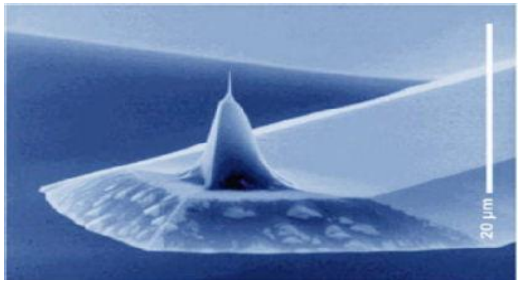

FM-DFM – Frequency modulation dynamic force microscopy

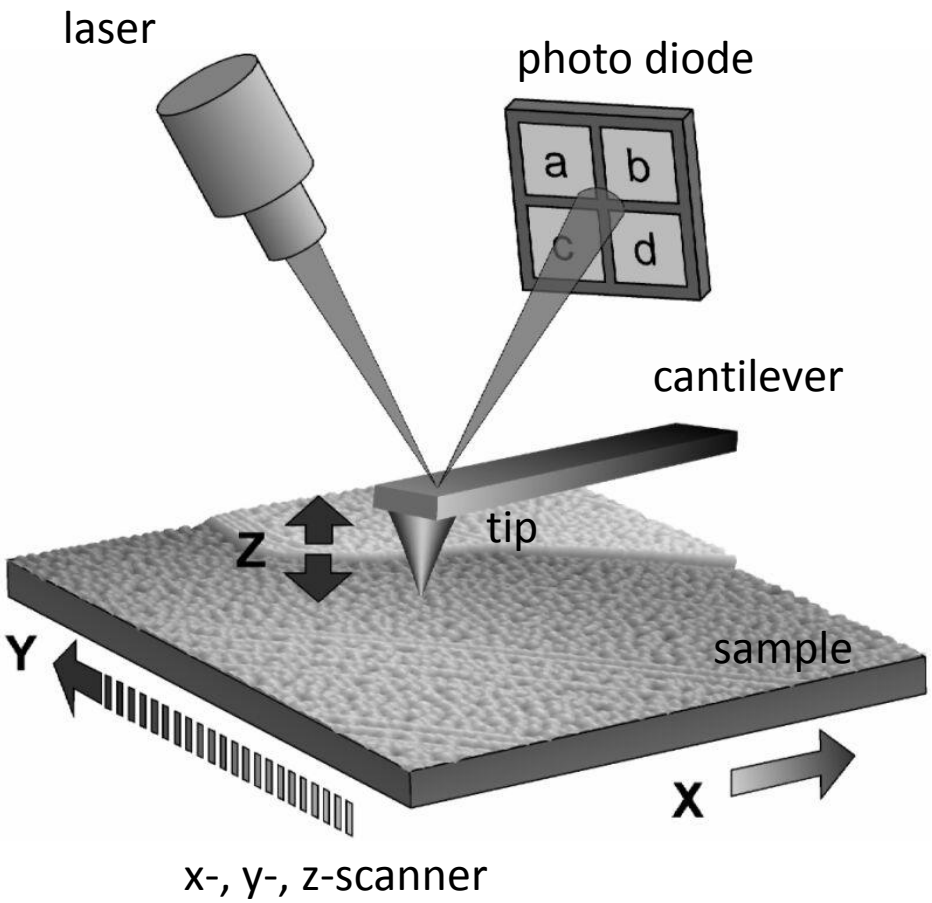

free oscillation of cantilever at its resonance frequency and amplitude

Approach to surface: influence of tip-sample interaction
⇒ frequency shift (const. amplitude)

Imaging: at constant frequency shift
(feedback controls tip-sample distance)

Force spectroscopy:
(Frequency shift vs. tip-sample distance)

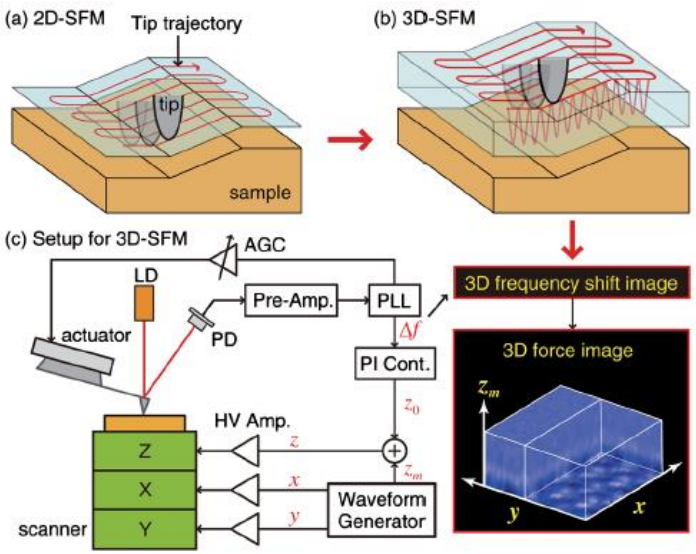

FM-DFM – Frequency modulation dynamic force microscopy (spectroscopy)

Muscovite mica (clay mineral) in contact with water

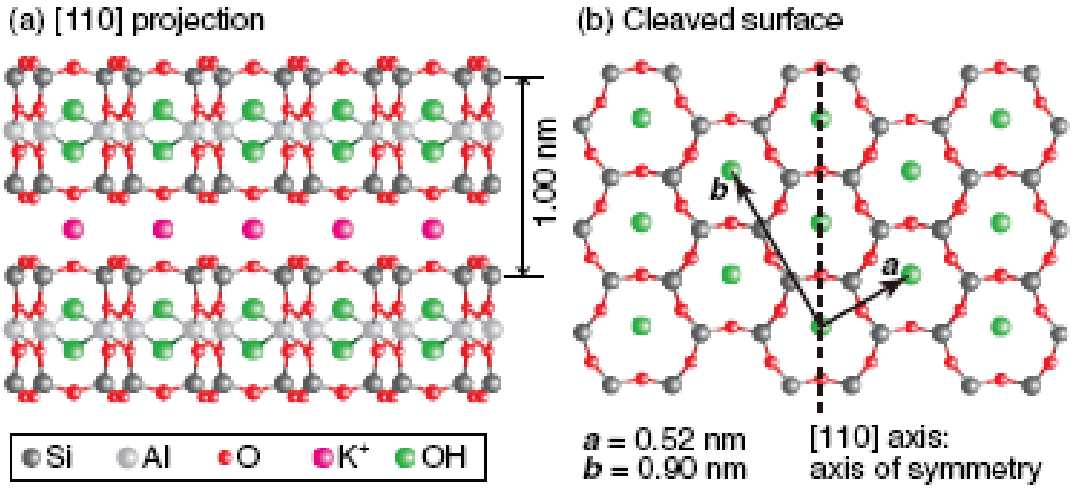

FM-DFM image in water

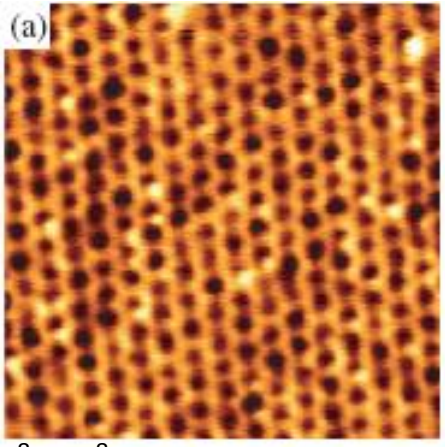

8 nm x 8 nm

Fukuma et al., Phys. Rev. Lett. 104 (2010) 106101.

FM-DFM – Frequency modulation dynamic force microscopy (spectroscopy)

Muscovite mica (clay mineral) in contact with water

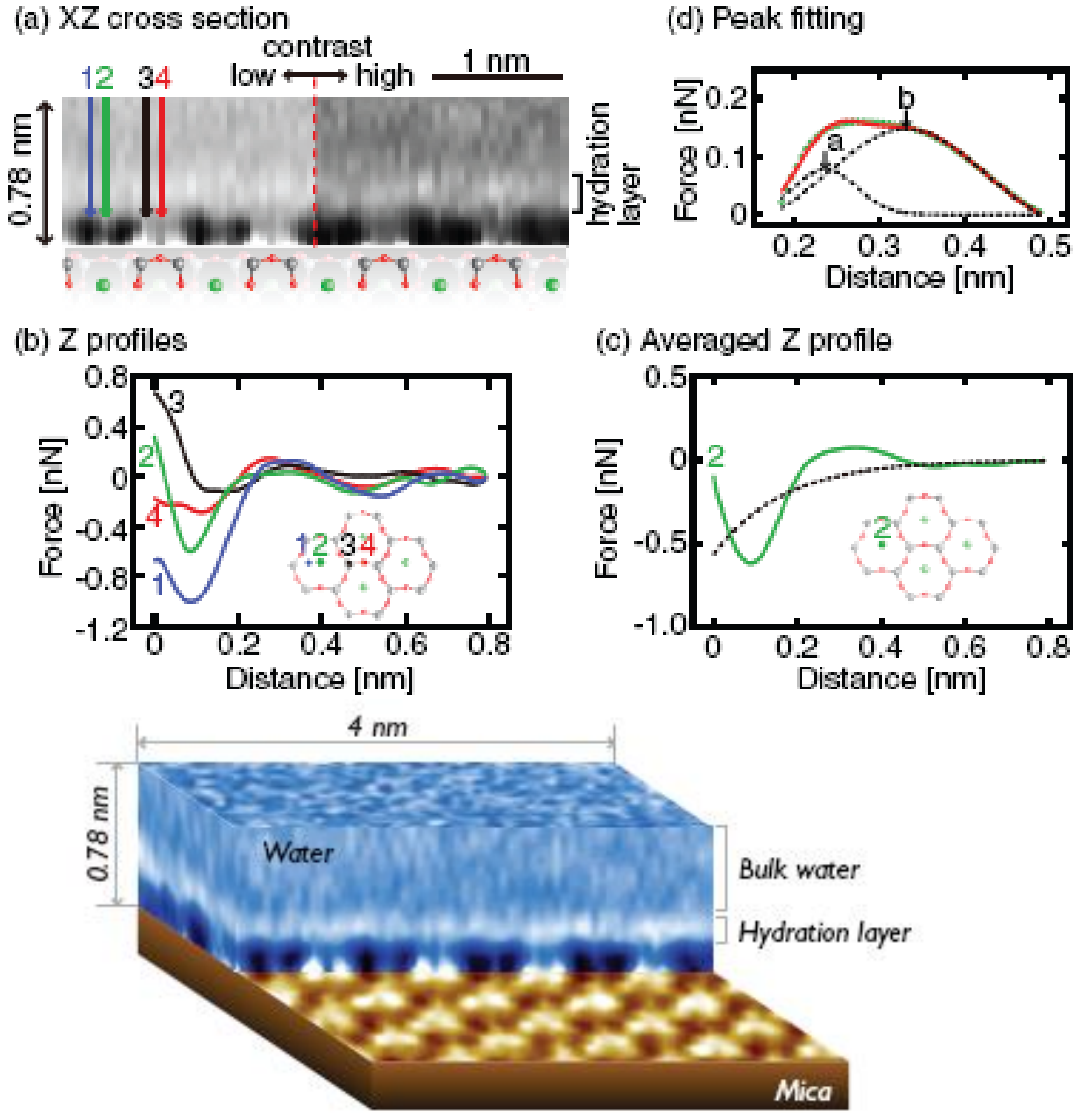

Fukuma et al., Phys. Rev. Lett. 104 (2010) 106101.

Park et al., Phys. Rev. Lett. 89 (2002) 085501.

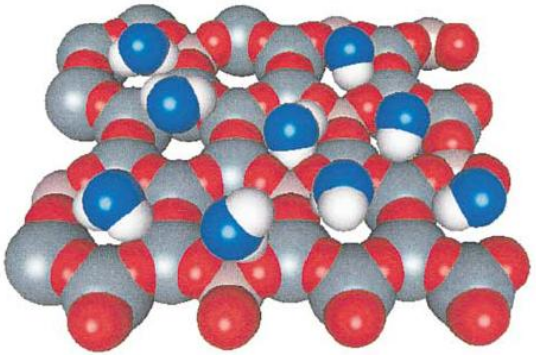

FIG. 2 (color). Perspective visualization of the adsorbed water molecules represented by peak *(a)* in Fig. 1 as predicted by MC simulation.

Water profile from X ray refl.

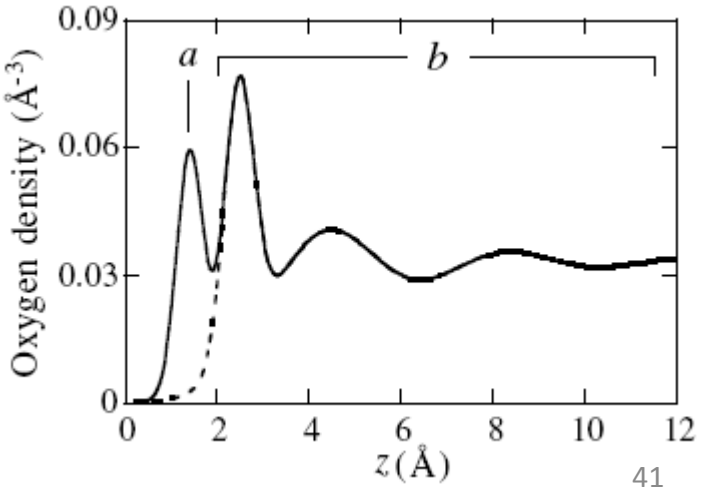

Cheng et al., Phys. Rev. Lett. 87 (2001) 156103.

Infrared spectroscopic methods

External reflection

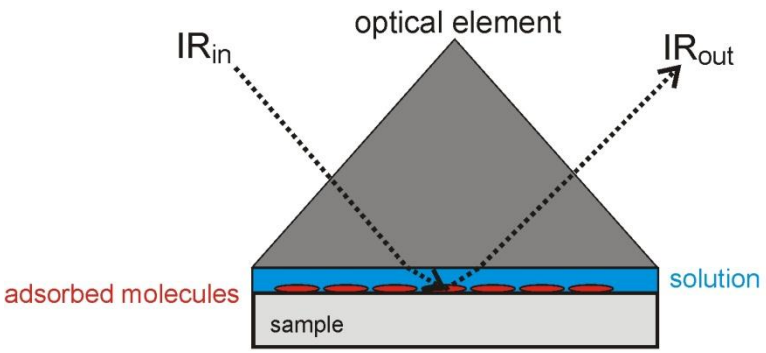

+ single crystalline surfaces
  - well defined surface crystallography

- thin layer cell (diffusion problems, resistence)
- electrolyte absorption (background)

Internal reflection

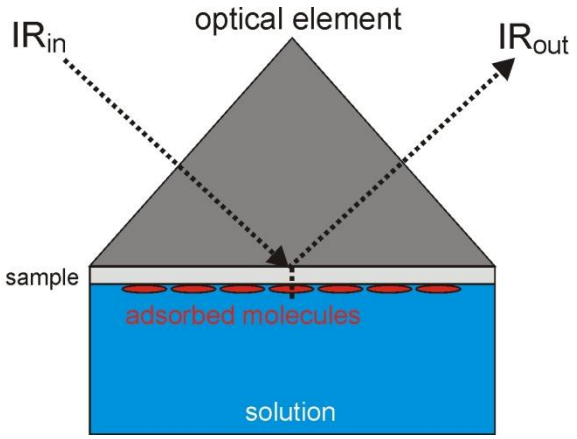

+ little solution contribution
+ no diffusion limitations (time-resolved measurements possible)
- surface morphology
- cleaning of internal reflection element

Surface selection rule

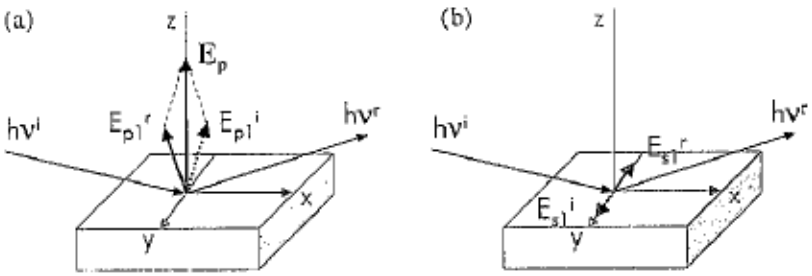

Fig. 9.3 Directions of the electric field vectors of the incident (dotted arrows) and the reflected (solid arrows) IR beams at the air/gold interface for (a) p-polarized and (b) s-polarized radiation.

Two limiting polaization states of the IR electric field vector:
E_p: parallel to the plane of incidence
E_s: perpedicular to the plane of incidence

at the metal surface:
electric field **enhancement** (constuctive interference between incident and reflected radiation) for **p-polarized** light at grazing incidence

electric field **cancellation** (destructive interference between incident and reflected radiation) for **s-polarized** light at all angles of incidence.

only the p-polarized part of the IR radiation may interact with dipoles on the surface.

air/Au interface

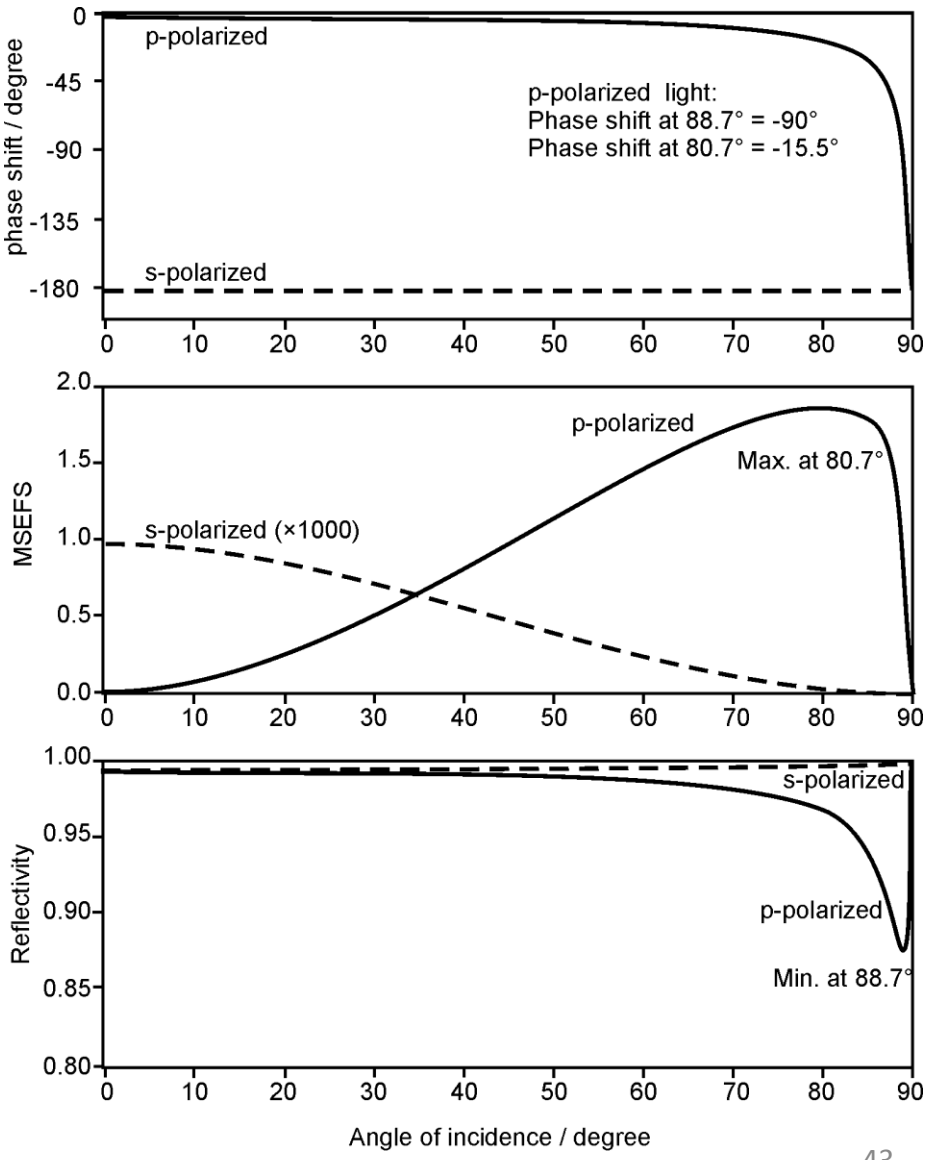

Zamlynny, Lipkowski, in: Adv. In Electrochem. Science and Engingeering, Vol. 9, Wiley, 2006

External reflection

Optimization of experimental conditions

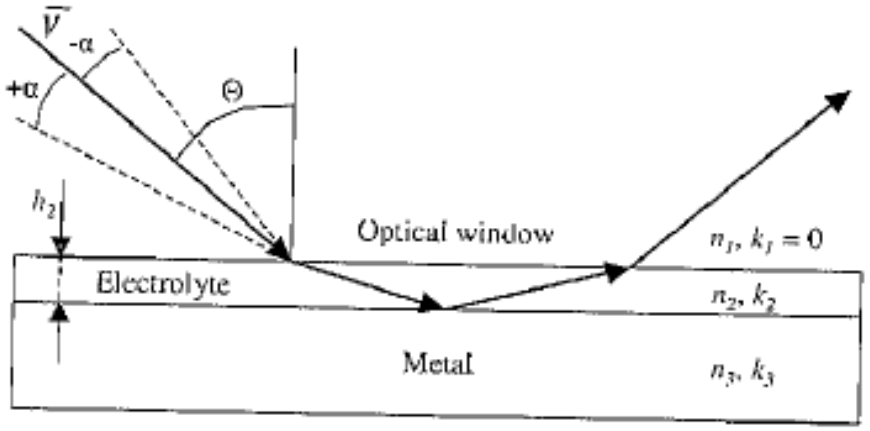

Fig. 9.4 Stratified medium that models the experimental thin-layer cell. $\bar{\nu}$, $\pm\alpha$ and Θ are the wavenumber, convergence and the angle of incidence of the infrared beam, respectively. n, k and h are the refractive index, attenuation coefficient and thickness of the three phases that comprise the stratified medium, respectively.

- Angle of incidence
- Thin cavity thickness
- Window material

Zamlynny, Lipkowski, in: Adv. In Electrochem. Science and Engingeering, Vol. 9, Wiley, 2006

External reflection

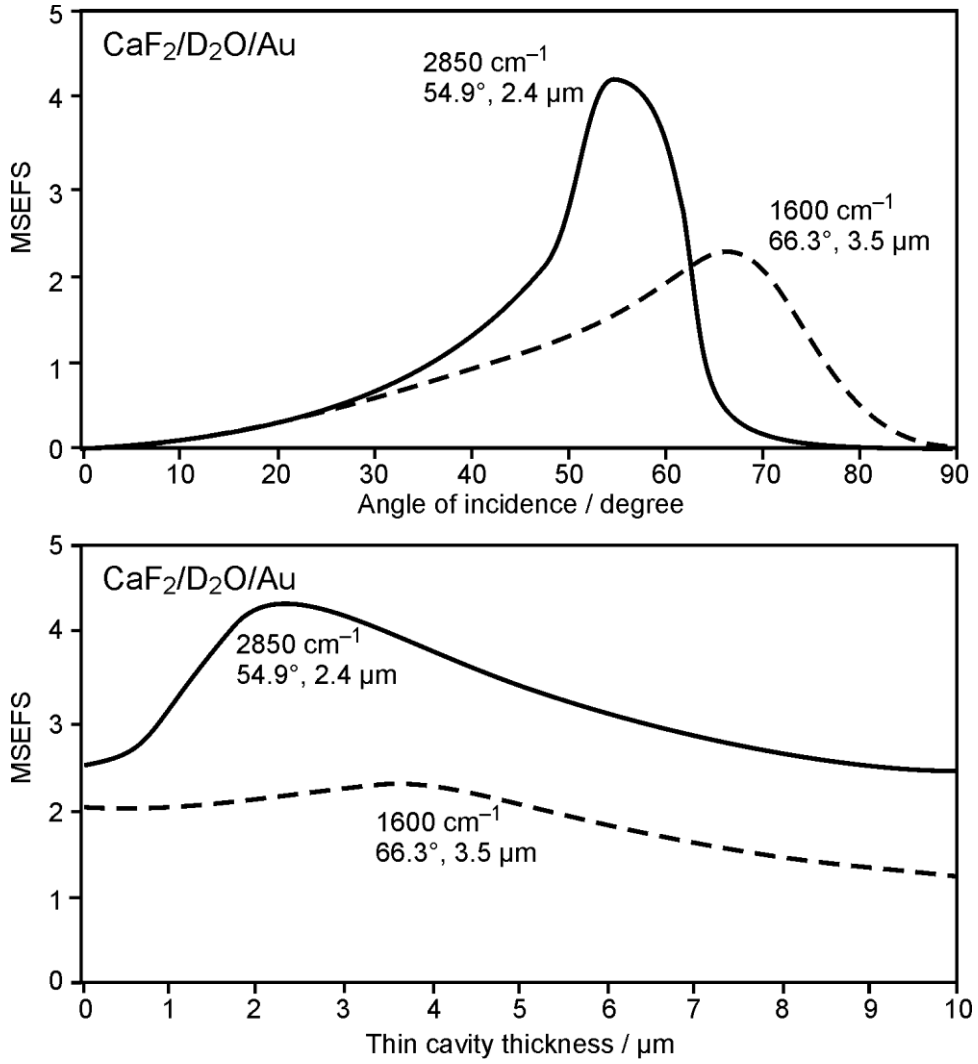

Zamlynny, Lipkowski, in: Adv. In Electrochem. Science and Engingeering, Vol. 9, Wiley, 2006

External reflection

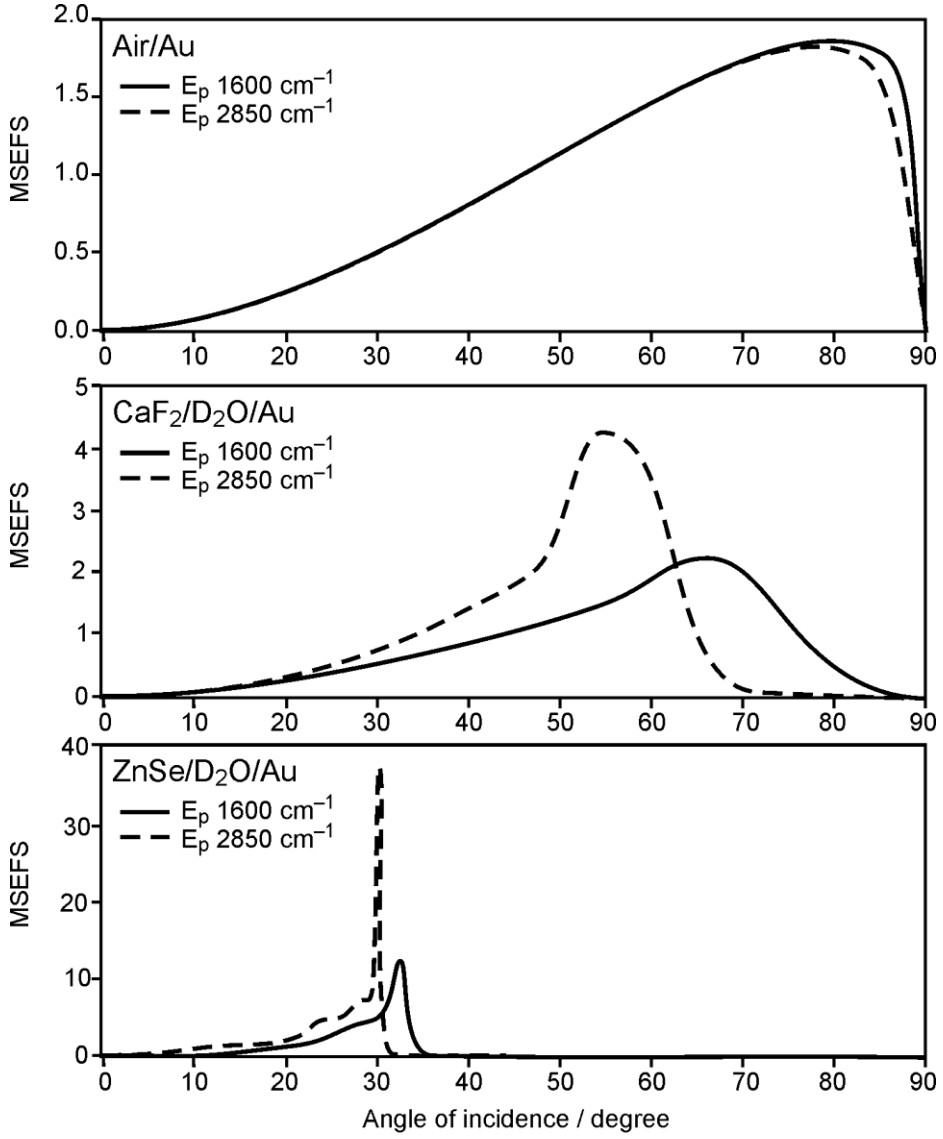

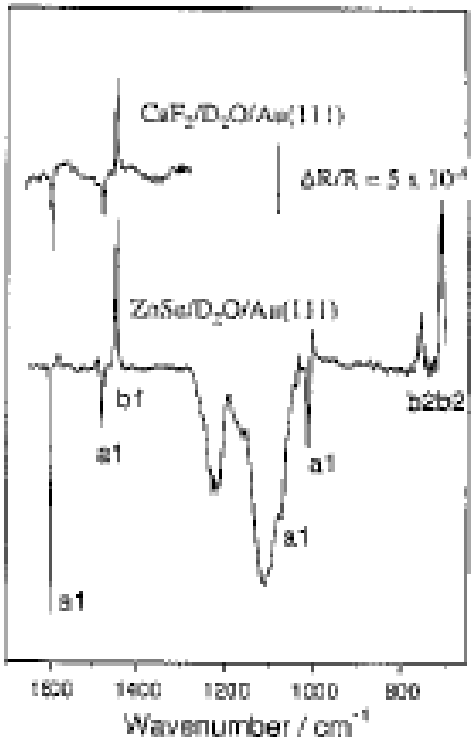

Fig. 9.10 Comparison of the SNIFTIRS spectra for pyridine adsorbed at an Au(111) electrode acquired using CaF_2 prism and ZnSe hemispherical windows. Taken with permission from Ref. [40].

Zamlynny, Lipkowski, in: Adv. In Electrochem. Science and Engingeering, Vol. 9, Wiley, 2006

External reflection

Main problem: electrolyte absorbs IR radiation

Solutions:

- *SNIFTIRS: Subtractively Normalized Fourier Transform Infrared Spectroscopy*

  Modulation of the electrode potential between the base value (E_1) and the sample value (E_2).

  Reflection absorption spectrum: $\frac{\Delta R}{R} = \frac{R(E_2) - R(E_1)}{R(E_1)}$ R_i: reflectivities

  Base potential at a value where the surface is free of adsorbed molecules.

- *Polarization dependent Infrared Reflection Absorption Spectroscopy*

- *Vibrational Sum Frequency generation (SFG) Spectroscopy*

Polarization dependent IRAS

-Static polarization switching: use linear polarizer and record s and p spectra separatly.

- Polarization modulation technique

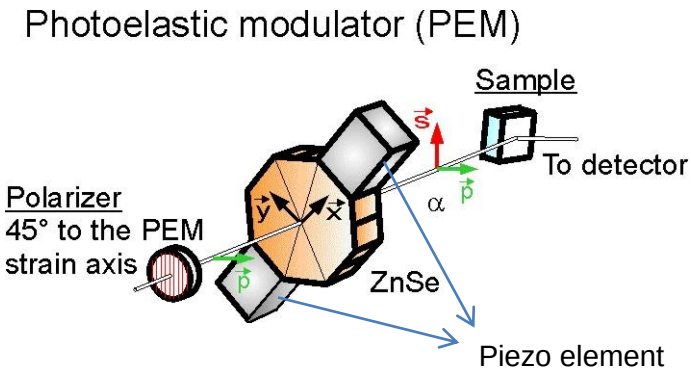

Piezo element converts a periodic voltage to a periodic mechanical wave, which compresses or expands the ZnSe crystal (at a frequency of 70 kHz).

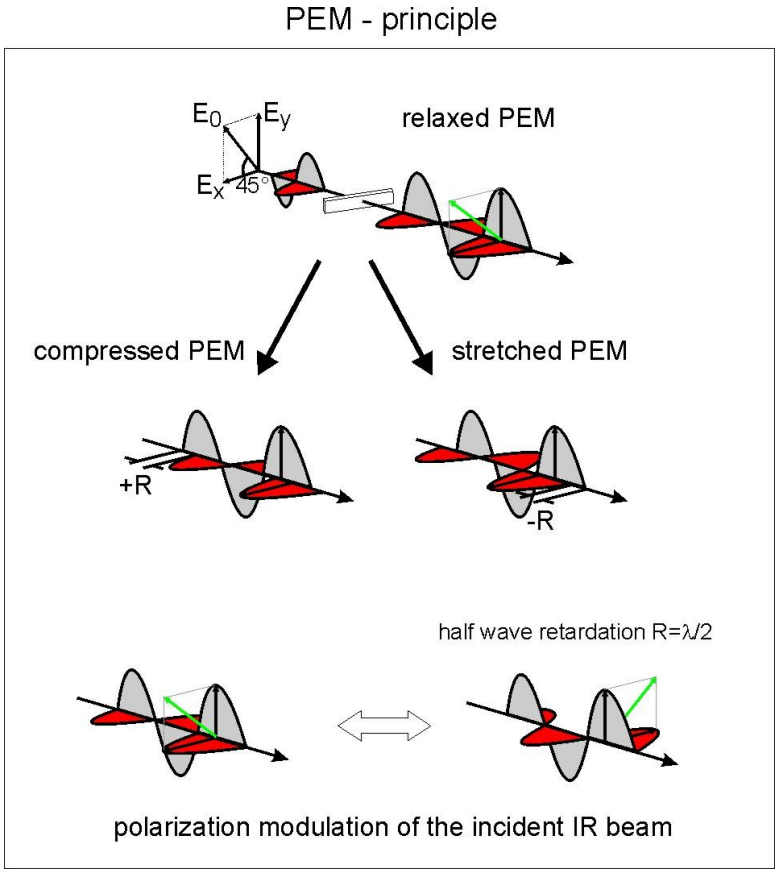

Surface selection rule: vanishing electric field of the s-polarized component at a metal surface.

with **p**-polarized component: detect **fluid phase** + **surface**
with **s**-polarized component: detect **only fluid phase**

Polarization dependent IRAS + (SNIFTIRS)

Anion adsorption on Pt(111)

Electrolyte: H_2SO_4 + Na_2SO_4

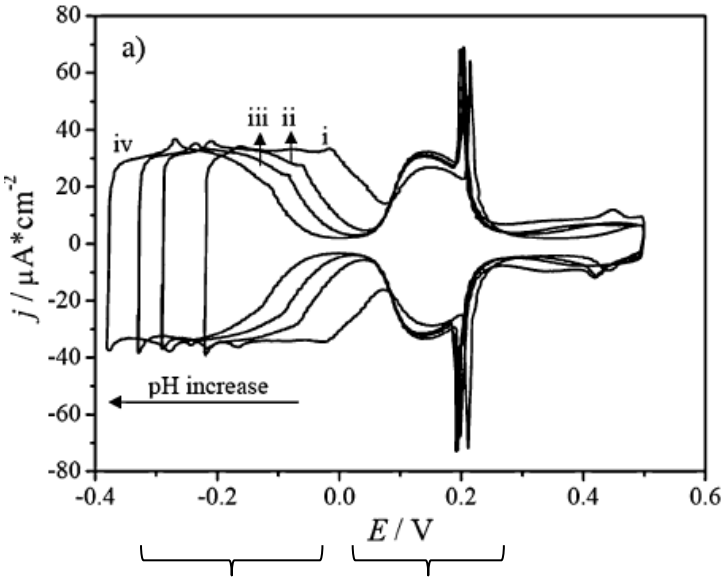

Hydrogen region anion adsorption/desorption
sulfate (SO_4^{2-}) or
bisulfate (HSO_4^-) or both?

IR: from p/s comparison

1250 cm^{-1}: adsorbed anion
1200 and 1100 cm^{-1}: solution species

p polarization s polarization

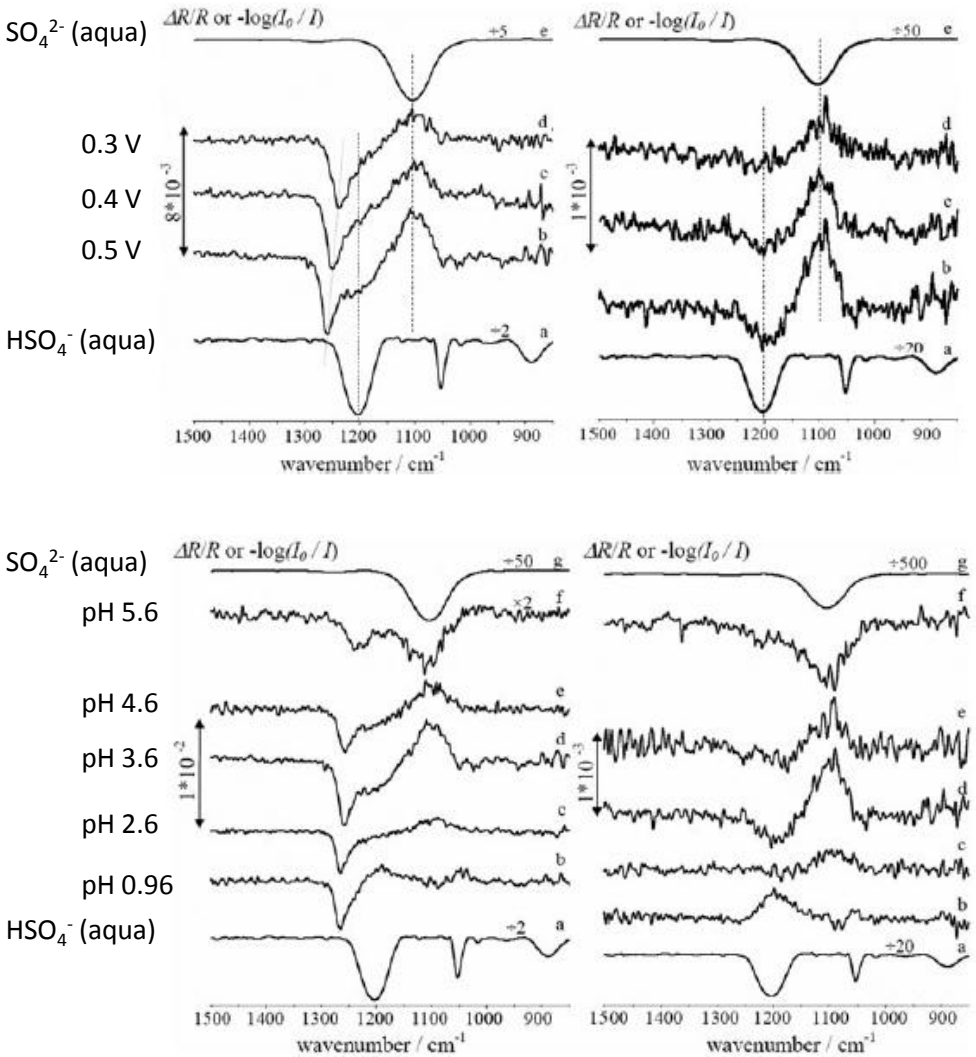

Su et al., PCCP 12 (2010) 15231.

Polarization dependent IRAS + (SNIFTIRS)

Anion adsorption on Pt(111)

Electrolyte: H_2SO_4 + Na_2SO_4

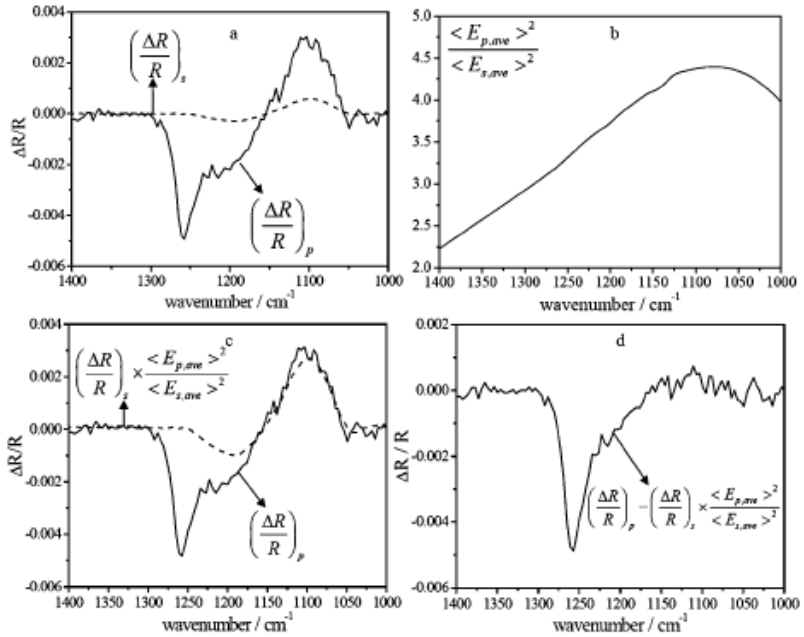

Fig. 4 (a) SNIFTIRS spectra of the Pt(111) electrode in 0.1 M Na_2SO_4 + 0.001 M H_2SO_4 solution at different polarized light, (b) variation of $\langle E_{p,\mathrm{average}}\rangle^2/\langle E_{s,\mathrm{average}}\rangle^2$ with wavenumber, (c) and (d) calculated IR spectra (indicated in the figure).

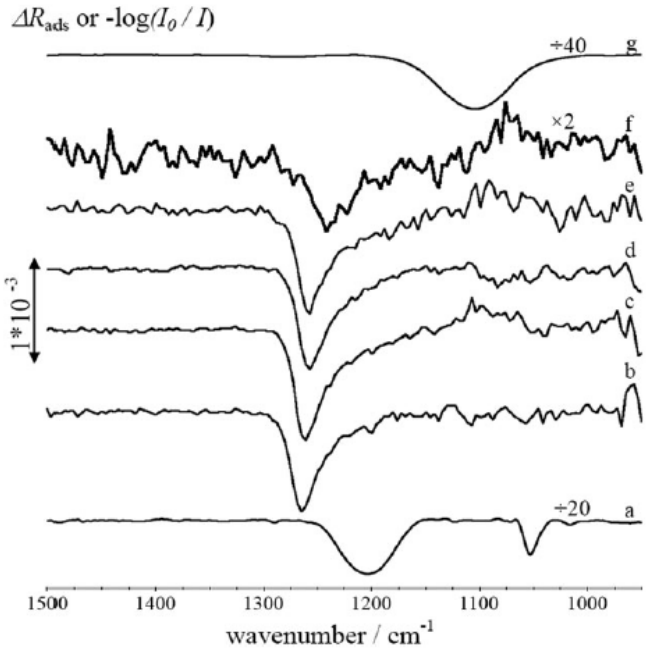

Fig. 5 ΔR_{ads} spectra of the Pt(111) electrode in solutions of different pH: (b) 0.96, (c) 2.6, (d) 3.6, (e) 4.6, (f) 5.6. (a) and (g) plot log I/I_o, the transmission IR spectra for 0.5 M K_2SO_4 + 3 M HCl and 0.5 M K_2SO_4 solution, respectively. E_S is 0.5 V for all the ΔR_{abs} spectra.

Conclusion: only sulfate adsorbed

$$\frac{\left\langle E_{p,avg}\right\rangle^2}{\left\langle E_{s,avg}\right\rangle^2}$$

ratio of MSEFS for p- and s-pol. radiation in the thin layer cavity

Su et al., PCCP 12 (2010) 15231.

CO adsorption on Pt(111)

Pt(111)-electrolyte

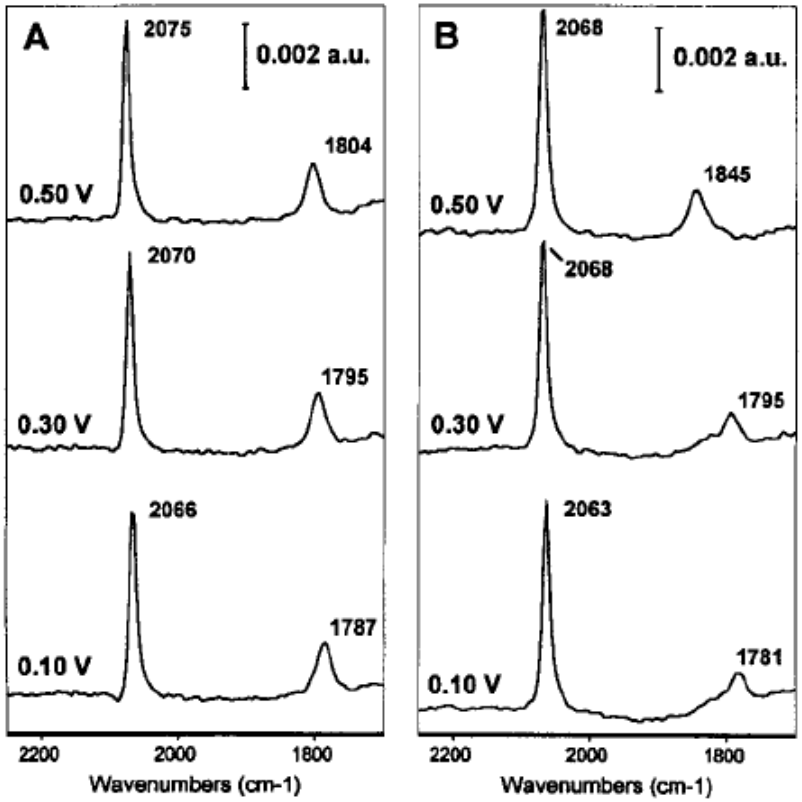

Rodes et al., Langmuir 16 (2000) 811.

Pt(111)-gas

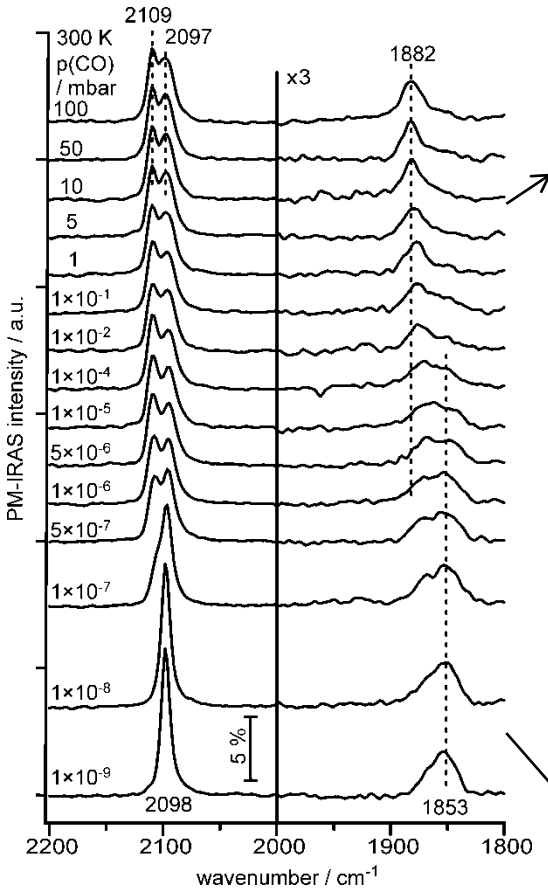

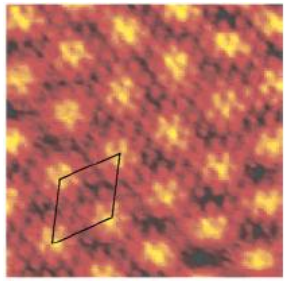

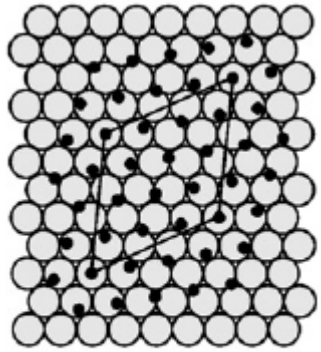

c) (√19×√19)R23.4
Moiré

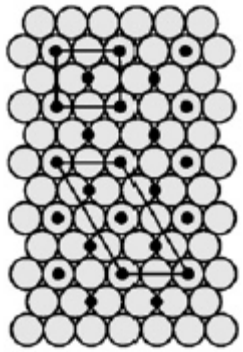

a) (2×√3)rect
= c(4×2)

Electrochemical Stark effect: frequency shifts with potential
Band positions lower in electrochemical environment : due to coadsorbed H_2O.
Two different CO species at lower frequency: 1781 cm^{-1} (3-fold hollow) and 1845 cm^{-1} (bridge)

CO adsorption on Pt(111)

Pt(111)-electrolyte

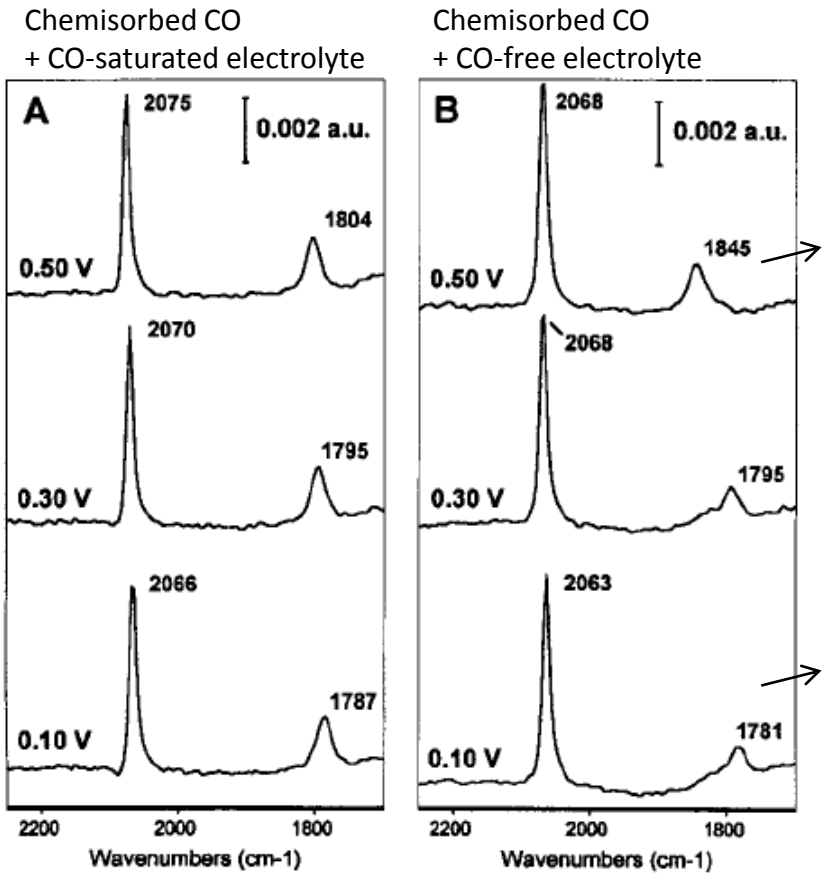

Rodes et al., Langmuir 16 (2000) 811.

(√19×√19)-13CO, θ=0.68 ML

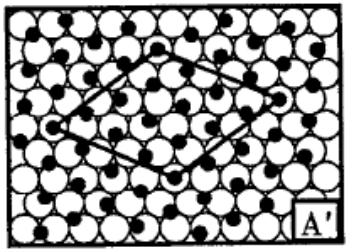

p(2×2)-3CO, θ=0.75 ML

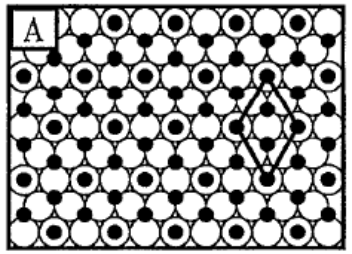

can only be stabilized in electrochemical environment

Two different CO species at lower frequency: 1781 cm^{-1} (3-fold hollow) and 1845 cm^{-1} (bridge)

CO oxidation on Pt(111)

$$CO_{ad} + OH_{ad} \rightarrow CO_2 + H^+ + e^-$$

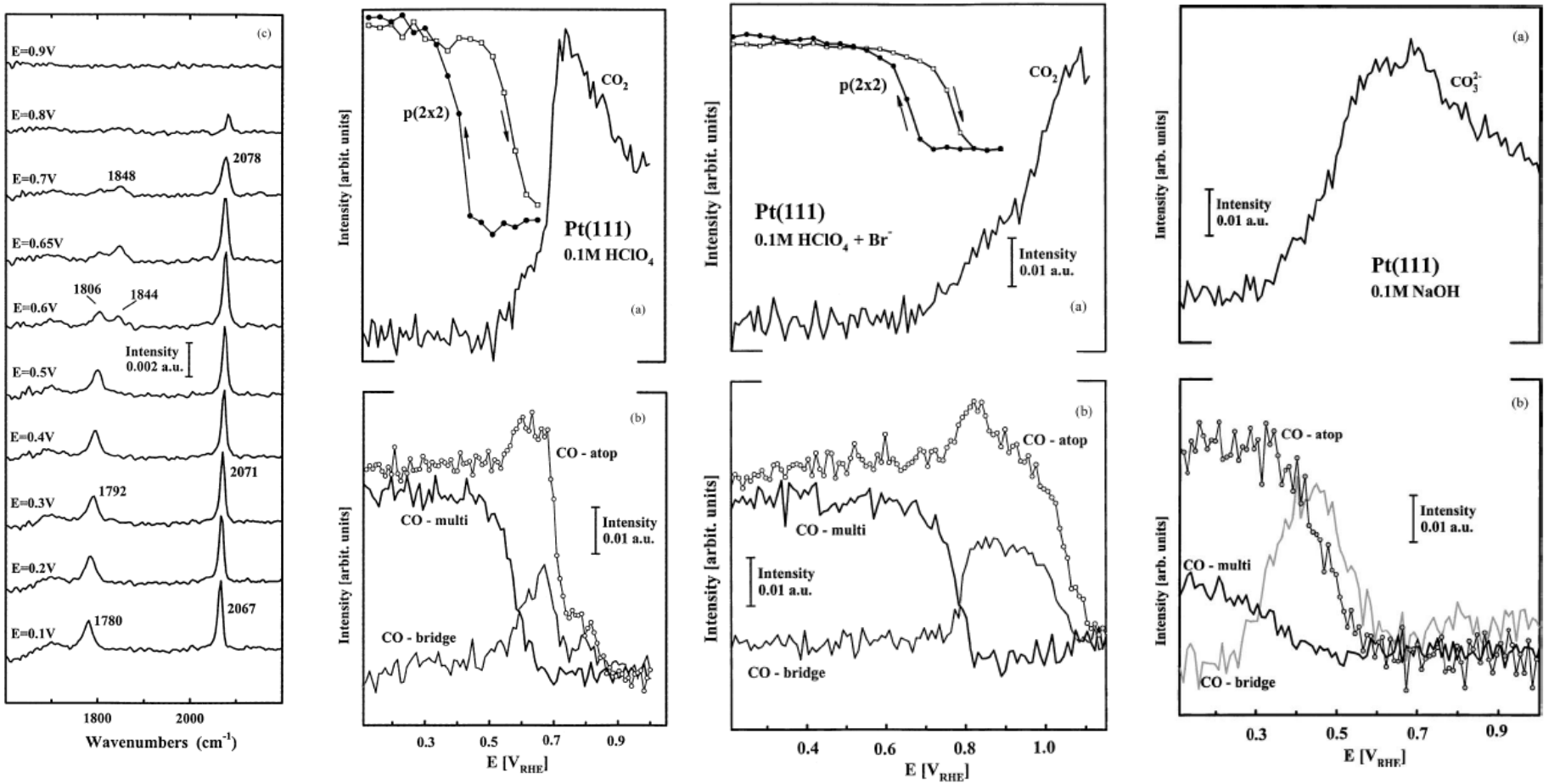

Possible reaction mechanism: weakly bound CO in p(2x2)-3CO structure reacts at low potential with OH adsorbed at defect/step sites. the remaining CO in (√19x√19)-13CO is strongly bound. Reaction at higher potential when OH adsorbs at terrace sites.

Influence of anions: Br^- selectively blocks step sites → higher onset potential for reaction.

Markovic & Ross, Surf. Sci. Rep. 45 (2002) 117.

Attenuated total reflection (ATR)

Total internal reflection (TIR)

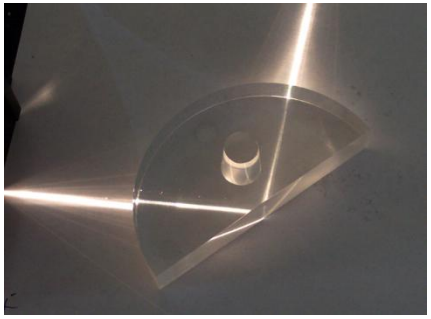

Internal reflection element: high refractive index (e.g. diamond, ZnSe, Ge, Si)

Angle of incidence > crtical angle

Light is reflected at the interface and forms an evanescent wave perpendicular to the total reflecting surface.

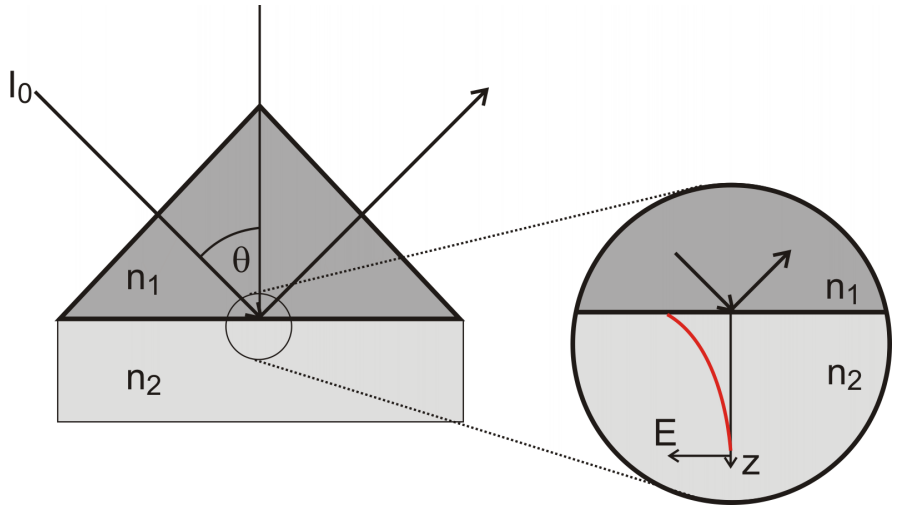

Critical angle: $\theta_c = \arcsin\left(\frac{n_2}{n_1}\right)$

Exponential decay of evanescent field into sample: $E = E_0 \exp\left(-\frac{z}{d_p}\right)$

Penetration depth: $d_p = \frac{\lambda}{2\pi\sqrt{\left(n_1^2 \sin^2\theta - n_2^2\right)}}$ 0.5 – 2 µm

Attenuated total reflection (ATR)

Deposition of catalyst

a) Thin metal film: Au, Ag, Pt,…. on IRE by physical vapor deposition
thickness of the film must be thinner than the penetration depth of the evanescent wave.
very homogeneous layers can be prepared

b) Powder catalyst
by dropping a slurry of catalyst on IRE and drying
e.g. Al_2O_3, TiO_2, silica, CeO_2
can be thicker than λ_p because of particulate nature

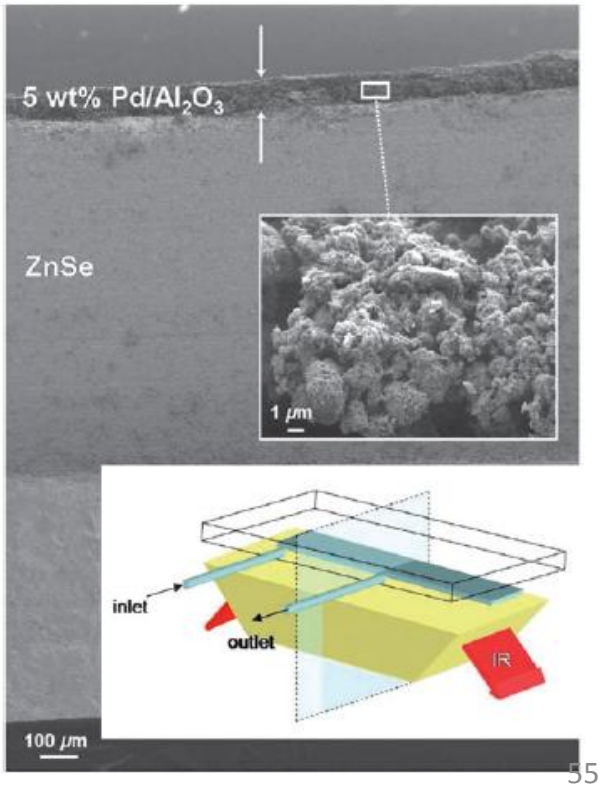

Andanson & Baiker, Chem. Soc. Rev. 39 (2010) 4571.

ATR - Surface enhanced infrared absorption spectroscopy (ATR-SEIRAS)

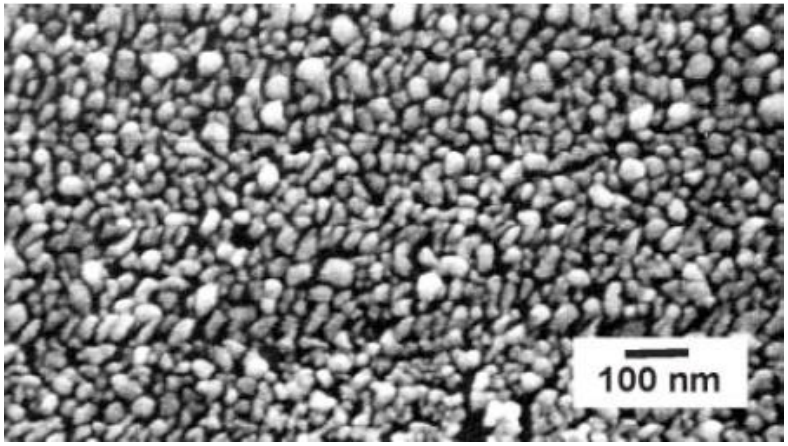

10 nm thick Ag film evaporated on Si (SEM image)

M. Osawa, Top. Appl. Phys. 81 (2001) 163.

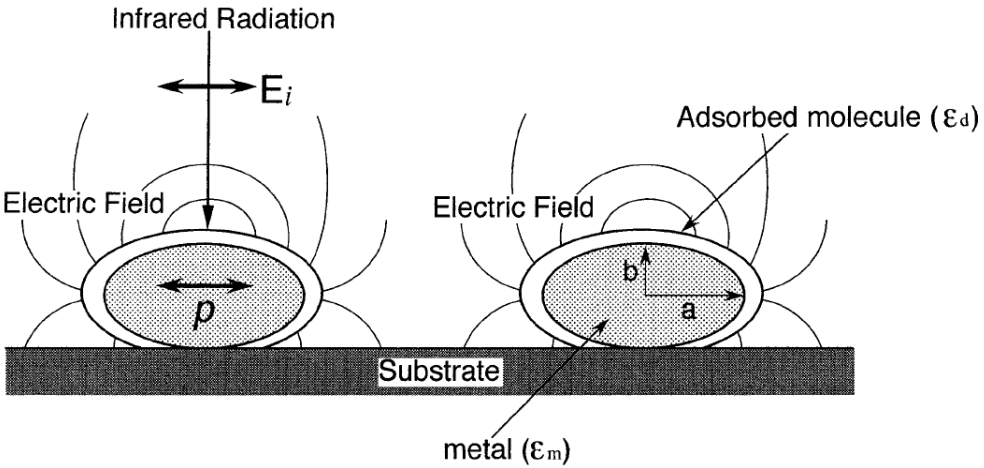

Metal particles are polarized by incident photon field → generates electromagnetic field that excites vibrations of adsorbed molecules. EM field at the surface up to 10 times larger than incident field.

EM field around particles is polarized along the surface normal at any point of the particles.

Surface selection rule identical to IRAS.

Distance dependence of electric field: r^{-3}

Enhancement is short-ranged and confined to adsorbed molecules.

$\Rightarrow$ possibility to detect interfacial water

ATR - Surface enhanced infrared absorption spectroscopy (ATR-SEIRAS)

Water on Au(111)-20 nm particles in 0.1 M H_2SO_4

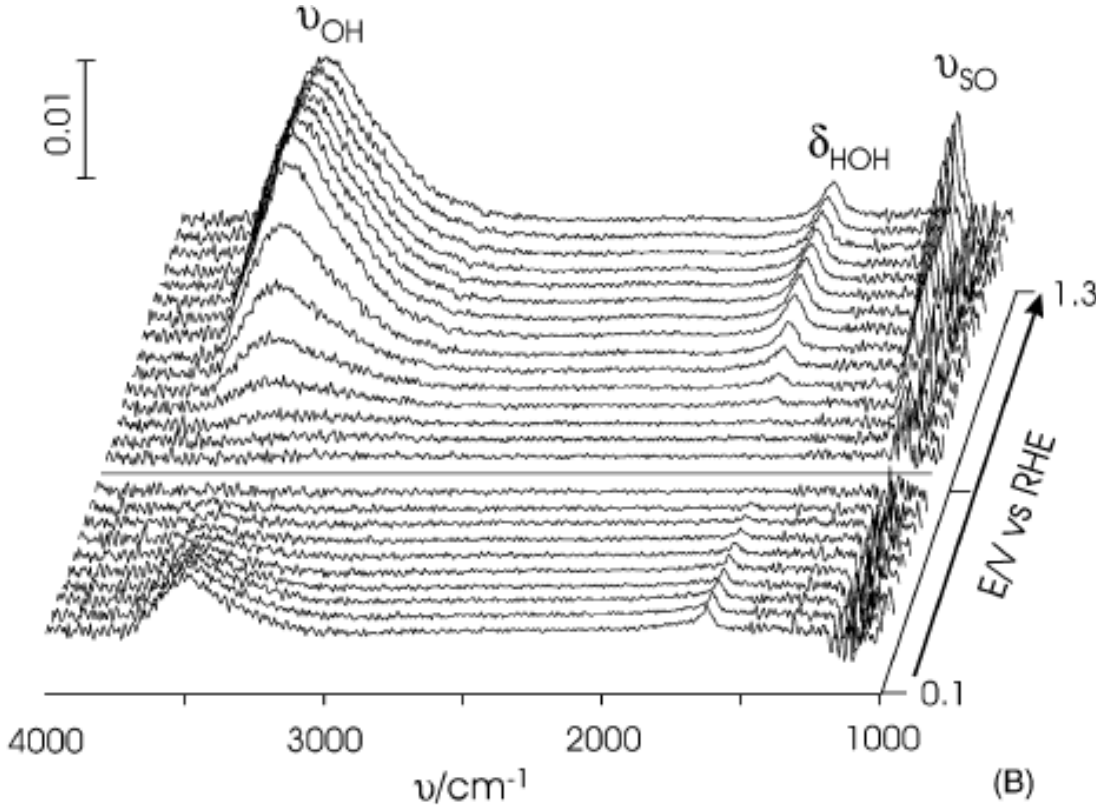

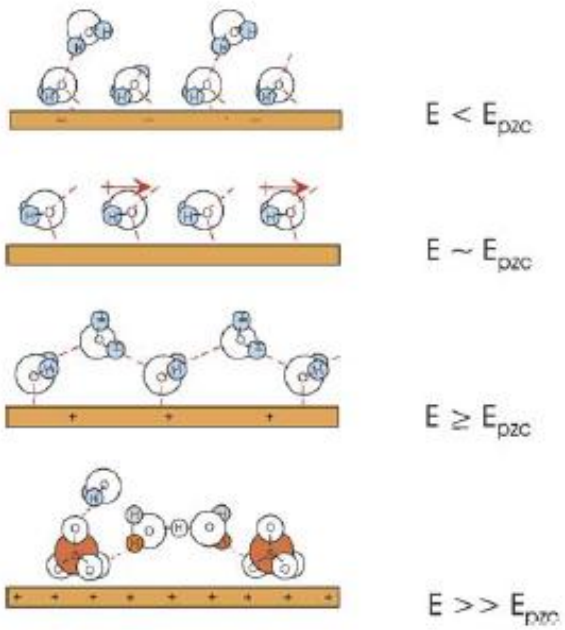

E_{PZC} = 0.55 V

Wandlowski et al., Electrochim. Acta 49 (2004) 1233.